environments

MDPI

Article

Microbial Responses to PFOA in Coastal Wetland: An Ecological Comparison Between Freshwater and Salt Marsh

Trang Vu [1], Maoqing Tian [1], Madhav Kharel [2], Weilan Zhang [2] and Yu Miao [1,3,*]

[1] Department of Civil and Environmental Engineering, Northeastern University, Boston, MA 02115, USA
[2] Department of Environmental & Sustainable Engineering, University at Albany, State University of New York, Albany, NY 12222, USA
[3] Department of Marine and Environmental Sciences, Northeastern University, Boston, MA 02115, USA
* Correspondence: y.miao@northeastern.edu

Abstract

Coastal wetlands provide critical ecosystem services yet face increasing per- and polyfluoroalkyl substance (PFAS) contamination, and comparison of wetland microbiome responses to PFAS remains poorly resolved. Laboratory-enriched microbial consortia derived from freshwater marsh and salt marsh soils were exposed to perfluorooctanoic acid (PFOA) in 75-day microcosms at 0, 1, and 10 mg/L, then characterized by 16S rRNA gene sequencing, phylogenetic null modeling, neutral community modeling, and KEGG-level functional prediction. Both enriched consortia showed a modest decrease in aqueous PFOA (~11–13%) at 1 mg/L but not at 10 mg/L, consistent with a potential contribution from biosorption-mediated immobilization. Incubation time dominated beta-diversity shifts (ANOSIM $R > 0.90$, $p = 0.001$), while PFOA produced no detectable compositional separation. Exploratory additive mixed-effects models indicated that alpha diversity varied primarily with microbial community source and sampling day, whereas PFOA concentration showed a nominal overall association only with Shannon diversity. Assembly analyses showed that PFOA was associated with stronger heterogeneous selection in the salt-marsh-derived consortium, whereas the freshwater-derived consortium remained stochastically dominated. When PFOA-exposed samples were pooled across both enriched consortia, the neutral community model fit collapsed ($R^2 < 0$), signaling a regime shift toward deterministic, PFOA-mediated selection. Functionally, the salt-marsh-derived consortium showed predicted enrichment in taurine/hypotaurine metabolism and broad-spectrum proteolytic functions (serralysin and creatinase), whereas the freshwater-marsh-derived consortium showed predicted enrichment in glutathione metabolism, xenobiotic dioxygenase functions, and DNA repair pathways. Candidate PFOA-sensitive (*Pseudohongiella*, *Flavobacterium*, *Parvibaculum*) and PFOA-tolerant (*Sericytochromatia*, *Legionella*) taxa were identified as source-associated candidate biomarkers. Under the tested culture conditions, PFOA responses differed between the laboratory-enriched freshwater-marsh- and salt-marsh-derived bacterial consortia. These results describe source-associated responses of the enriched consortia but may need further validation with native wetland communities.

Keywords: perfluorooctanoic acid (PFOA); coastal wetland microbiome; community assembly; neutral community model; functional prediction; ecological biomarker

Check for updates

Academic Editors: Panagiotis Papazotos, Eleni Gianni and Dionisios Panagiotaras

Received: 15 September 2026
Revised: 27 October 2026
Accepted: 28 October 2026
Published: 3 November 2026

Copyright: © 2026 by the authors. Licensee MDPI, Basel, Switzerland. This article is an open access article distributed under the terms and conditions of the Creative Commons Attribution (CC BY) license.

1. Introduction

Coastal estuarine wetlands occupy the interface between marine and terrestrial environments, including mangroves, seagrass beds, and marshes [1]. Among them, freshwater

and salt marshes are particularly important ecosystems because of high productivity and fast sediment deposition, and are valued for storm buffering, nutrient cycling, carbon storage, flood attenuation, water purification, and shoreline stabilization [2]. Together, these ecosystem functions support diverse plants, animals, and microbial communities and contribute to wetland biodiversity [3]. Hydrological and geological processes are among the main drivers shaping subsurface salinity, plant productivity, and the consequent ecological functions of coastal wetlands [4,5]. Under climate change, marshes with accretion rates slower than the rate of sea level rise are susceptible to inundation and submergence [6,7]. Freshwater marshes may migrate landward and be replaced by salt marshes as saltwater intrusion progresses [8]. On the other hand, terrestrially derived freshwater inputs are increasingly recognized as important sources of water and solutes to intertidal wetlands and salt marshes [9].

One of the main functions of coastal wetlands is to regulate the essential biogeochemical cycles, including organic matter decomposition, nutrient cycling, and gaseous exchanges. The soil microbiomes that inhabit these transitional terrestrial–aquatic zones experience regular or irregular inundation and pronounced gradients in structural heterogeneity, water content, pH, salinity, and organic matter [10], which affect the composition and function of microbial communities [11]. Extended flooding drives the sediments anoxic and slows organic matter decomposition [12]. In response, microbial communities accumulate biomass and accelerate the biogeochemical processes they control. The soil microbiomes have the capacity to decompose soil organic matter, facilitate sulfate reduction, oxidize sulfide/sulfur, reduce iron, perform nitrification, degrade contaminants, and contribute to the improvement of soil structure and ecosystem stability [13]. Metabolic allocations towards traits that enhance stress tolerance, such as the production of extracellular polymeric substances (EPS), may inadvertently bolster carbon sequestration [14]. Additionally, microbial biochemical pathways are acutely responsive to environmental stresses, with microbial communities exhibiting reduced uptake of plant-derived carbon under conditions of heat and drought [15]. Nutrients are one of the main factors determining the activity of microbial communities and processes that regulate decomposition and nutrient cycling rates in the oligotrophic zones of coastal wetlands [16]. However, freshwater waterways can be a major source delivering nutrients from upstream, and it has been found that some archaeal groups are organo-heterotrophic for particular carbohydrates and dissolved carbon in coastal wetlands [17]. Thus, the material exchange between freshwater and salt marshes creates a dynamic ecosystem with a variety of resources (nutrients, substrates, and electron acceptors) and surroundings (such as oxygen levels and pH). Heterogeneity in resources and surroundings has a significant impact on competition between species, and diversity varies from that observed under homogeneous conditions. These changes in community richness and diversity ultimately impact ecosystem functions at the regional or global level [18].

Beyond these natural drivers, coastal ecosystems are also highly vulnerable to anthropogenic disturbance [19]. For centuries, coastal wetlands and human populations have been closely intertwined, and many of these ecosystems have been progressively replaced or fragmented by agriculture, aquaculture, industry, and tourism [6]. A critical knowledge gap remains regarding the accumulation dynamics of anthropogenic compounds, such as organochlorine pesticides (OCPs), microplastics (MPs), per- and polyfluoroalkyl substances (PFASs), and polychlorinated biphenyls (PCBs). These contaminants are recognized as emerging but persistent pollutants in coastal marshes and their resident microflora [1]. Among pollutants, PFASs have become ubiquitous contaminants detected globally in soil, groundwater, surface water, sediments, and biota [20,21]. They have drawn attention because of their ecological, animal, and human toxicity [22–25], as well as enhanced mobility,

resistance to degradation [26], bioaccumulation [27], environmental persistence [28], and long-range transport potential [29]. In coastal areas, the impacts of these contaminants on microbial communities and the subsequent ecological reverberations remain less understood than in other ecosystem types. This gap represents a critical frontier for environmental sustainability and management [30,31].

PFAS compounds have been reported to alter microbial composition, diversity, and function across diverse environments [32], whereas their biotransformation remains poorly understood owing to the difficulty of cleaving the C–F bond. Long-term PFAS exposure has been shown to significantly decrease the biodiversity of soil microbial communities and to enrich PFAS-tolerant lineages, such as *Pseudomonadota*, *Acidobacteriota*, and *Bacteroidota* [33,34]. Carbohydrate metabolism, global/overview maps, and membrane transport pathways in soil microbes are also affected by PFAS stress. Glycosyltransferases in PFAS-polluted soils were upregulated, whereas glycoside hydrolases were severely inhibited [32]. PFAS-induced perturbations to microbial community structure or function therefore carry the risk of unstable ecosystem services [33,35–38]. Field and microcosm studies have demonstrated that PFAS stress can disrupt nitrogen cycling by inhibiting genes involved in nitrification and denitrification [39,40]. Carbon cycling is similarly perturbed: PFAS exposure has been reported to transiently stimulate litter decomposition and β-glucosidase activity while inhibiting soil respiration and carbohydrate-related metabolism [37,41]. Among thousands of PFAS compounds, perfluorooctanoic acid (PFOA) is one of the most detected long-chain PFAS [42]. Owing to its extreme chemical stability, PFOA resists biotic and abiotic degradation and persists in aquatic and terrestrial environments, posing a non-negligible threat to organisms. Because coastal wetlands are heterogeneous environments increasingly affected by human activity and climate change, their indigenous microbial communities can develop high diversity and functional stability [43]. Together, these properties regulate ecosystem services and sustain water purification functions [13,44]. However, whether distinct microbial community structures emerge in coastal wetlands under PFAS stress, and what mechanisms underpin microbial resilience or adaptation, remain understudied.

To address these knowledge gaps, the present study compared the bacterial community composition, assembly patterns, and predicted functions of laboratory-enriched microbial consortia derived from freshwater marsh and salt marsh soils under PFOA exposure. The hypothesis was that the responses of these two enriched, soil-derived consortia to PFOA would depend on their inoculum source and corresponding culture conditions. To test this hypothesis, microcosms inoculated with laboratory-enriched microbial consortia derived from freshwater marsh and salt marsh soils were incubated under three PFOA concentrations (0, 1, and 10 mg/L) for 75 days, with periodic sampling for 16S rRNA gene sequencing and PFOA quantification. The study was not designed to reproduce or predict the responses of intact wetland communities under field conditions, but instead described the compositional trajectories of the enriched consortia under PFOA exposure.

2. Materials and Methods

2.1. Study Site

The soil samples were collected along the Neponset River in the Boston area, Massachusetts, USA. The Neponset River Estuary is the section of the river where freshwater and saltwater mix, hosting 600 acres of salt marshes, managed as the Neponset River Reservation. The landward extent of the estuarine portion of the Neponset River is defined by a dam [45], and the flow is gauged by the US Geological Survey at a location just downstream from the dam to indicate the freshwater flow [46]. To capture the freshwater marsh-versus-salt marsh contrast, soil samples were collected from the freshwater marsh immediately downstream of the Baker Dam and from the salt marsh near the river mouth at Dorchester Bay, Boston

Harbor (Figure S1). At both the freshwater marsh and salt marsh sites, sampling was performed at low tide within the low-marsh landscape. Soil from the 0–30 cm layer was collected at three spatially separated locations within each sampling area. The soil collected from the three locations at each site was combined and homogenized to form one composite soil sample representing that site. Background PFOA concentrations and site-specific salinity, pH, electrical conductivity, redox potential, organic carbon, and nutrient concentrations were not measured. The elevation difference between the freshwater marsh and the salt marsh is 12.71 m, and the straight-line distance between the sites is 3019 m.

2.2. Soil-Derived Microbial Inoculum Preparation

The microbial inoculum was prepared from the homogenized composite soil. The surface runoff collected from the same site was filtered before use to remove microorganisms and was included to provide site-derived dissolved environmental constituents during microbial extraction. Therefore, the microbial component of the resulting inoculum was derived from the composite soil. A 10 g subsample of the homogenized composite soil and 15 mL of filtered surface runoff from each site were added to 50 mL of phosphate-buffered saline (PBS) containing 0.25% (*w*/*v*) sodium pyrophosphate, then vortexed to release bacterial cells from soil particles under neutral-pH buffering. Low-speed centrifugation at 500× *g* was used to pellet coarse debris while retaining microbial cells in the supernatant. The settled debris was washed another three times, and all supernatants were collected. The pooled supernatants were then passed through 70-µm cell strainers to remove residual particles and larger fungal hyphae and propagules. This procedure was selected to generate a particle-reduced bacterial inoculum suitable for subsequent liquid cultivation. Sodium pyrophosphate was used as a chemical dispersant to promote the release of cells from soil aggregates, while vortex mixing and low-speed centrifugation were used to separate suspended cells from coarse soil particles [47–49]. These procedures preferentially recovered free and loosely particle-associated bacteria but provided incomplete recovery of tightly particle-associated microorganisms [48,49]. Because the study focused on bacterial community responses using 16S rRNA gene sequencing, the preparation and subsequent analyses were designed to characterize the bacterial component of the enriched consortia rather than the complete soil microbiome. Fungi, archaea, protozoa, and other eukaryotic microorganisms were not characterized, and their presence or responses could not be evaluated.

2.3. Microcosms Setup

The microcosms were established in 250-mL serum bottles containing 100 mL of culture and approximately 150 mL of ambient-air headspace. The bottles were opened in a biosafety cabinet during each sampling event and were therefore periodically re-aerated. Dissolved oxygen was not monitored during the 75-day incubation; consequently, oxygen availability between sampling events could not be reconstructed. Standard ammonium mineral salts (AMS) medium was prepared based on the formulation reported by Omer et al. (2004) [50]. The basal medium contained, per liter, 0.70 g K_2HPO_4, 0.54 g KH_2PO_4, 1.00 g $MgSO_4{\cdot}7H_2O$, 0.20 g $CaCl_2{\cdot}2H_2O$, 4.0 mg $FeSO_4{\cdot}7H_2O$, 0.50 g NH_4Cl, 100 µg $ZnSO_4{\cdot}7H_2O$, 30 µg $MnCl_2{\cdot}4H_2O$, 300 µg H_3BO_3, 200 µg $CoCl_2{\cdot}6H_2O$, 10 µg $CuCl_2{\cdot}2H_2O$, 20 µg $NiCl_2{\cdot}6H_2O$, and 60 µg $Na_2MoO_4{\cdot}2H2O$, with thiamine supplied as a vitamin supplement [50], and the pH was adjusted to 6.8. A carbon mixture was supplied to both media and contained 2 mM sodium acetate, 1.33 mM sodium propionate, 0.67 mM each of sodium benzoate, p-hydroxybenzoate, glucose, and cellobiose, and 0.167 g/L each of yeast extract and tryptone. The mixture provided organic acids, aromatic compounds, carbohydrates, and complex organic nutrients and was used to represent the organic carbon

supply associated with soil total organic carbon (TOC) and to maintain microbial growth after the cells were separated from the soil matrix. Carbon availability can limit soil bacterial growth, while substrate composition and concentration can affect the recovery of heterotrophic soil microorganisms in culture. Providing this carbon mixture was therefore intended to limit community changes caused by carbon deprivation during enrichment. Defined AMS media were selected instead of filtered estuarine water to maintain known and reproducible concentrations of mineral nutrients, vitamins, and mixed carbon substrates across the PFOA treatments. Natural seawater varies spatially and temporally in its inorganic nutrients and dissolved organic matter, whereas defined artificial seawater media reduce batch-to-batch variation and improve the reproducibility of marine microbial cultivation [51,52]. Marine AMS medium is an established defined medium for cultivating microorganisms from marine sources and is commonly supplemented with 20–30 g/L NaCl [51,53], and a formulation containing 20 g/L NaCl has also been used to cultivate the model marine bacterium *Ruegeria pomeroyi* DSS-3 [53]. Accordingly, standard AMS without added NaCl was used for the freshwater-marsh-derived cultures, whereas marine AMS containing 20 g/L NaCl was used for the salt-marsh-derived cultures. The purpose was to provide standardized nutrient conditions within each source-derived culture series and a reproducible salinity contrast across the PFOA treatments rather than to recreate the complete site-specific chemistry of estuarine water. Soil-derived microbial inocula (5 mL) were diluted into the appropriate AMS medium (95 mL) at a 1:20 dilution, and biomass was monitored by optical density at 600 nm (OD_{600}) to follow growth. When the cultures reached stationary phase (5–7 days), the suspensions were transferred into fresh medium and cultivated again. This passaging was repeated three times as a pre-exposure enrichment step to select microorganisms capable of sustained growth in standard AMS for the freshwater-derived inoculum and marine AMS supplemented with 20 g/L NaCl for the salt-marsh-derived inoculum, thereby generating controlled starting consortia for the subsequent PFOA exposure experiment. Serial enrichment and transfer in defined media are established approaches for producing simplified and comparatively stable microbial consortia suitable for controlled experiments [54–56]. At the same time, this selection process progressively diluted and removed some low-abundance taxa that could not maintain growth under the supplied culture conditions [55–59]. The enriched microbial suspension (100 mL) was then transferred into 250-mL serum bottles sealed with butyl rubber stoppers for microcosm setup. This enrichment-based design provided controlled starting communities for comparison across PFOA treatments, while direct exposure of intact field communities in their native matrices was beyond the scope of the experiment. The resulting cultures are hereafter referred to as laboratory-enriched microbial consortia derived from freshwater marsh and salt marsh soils. These consortia originated from natural soil inocula but were subsequently shaped by microbial cell extraction, cultivation in defined media, and three serial transfers. They therefore represent cultivation-selected subsets of the source communities rather than intact wetland microbiomes. The original freshwater and salt marsh soils may have differed in microbial biomass and soil characteristics. Because this was a microbe-driven study, microbial cells were extracted from the soils and cultivated in defined media to minimize the influence of these differences on the subsequent PFOA comparison. PFOA was obtained as a certified perfluoro-n-octanoic acid reference solution (CAS No. 335-67-1; molecular weight, 414.07 g/mol; Wellington Laboratories Inc., Guelph, ON, Canada; lot PFOA0824). The chemical purity was >98%, and the supplied solution had a certified concentration of 50.0 ± 2.5 µg/mL in methanol containing <1% water. According to the certificate of analysis, the reference solution also contained four molar equivalents of NaOH. The supplied 50 mg/L solution was used as the primary stock and was sequentially diluted to 5 mg/L and 100 µg/L with sterile ultrapure water. Appropriate volumes of the

stock and working solutions were added to obtain nominal PFOA concentrations of 0, 1, and 10 mg/L. The 1 and 10 mg/L treatments were selected as elevated experimental exposures, and the two levels provide a 10-fold concentration contrast. They also span the range of concentrations used in previous freshwater microbial community experiments [60,61]. These concentrations were not intended to reproduce background PFOA concentrations at the sampling sites. Without the carbon mixture, carbon limitation could have caused greater changes in community composition during enrichment [62,63]. Abiotic controls were prepared identically and then autoclaved to eliminate microbial activity while preserving the same chemical matrix. Each PFOA treatment condition was established in three biological replicate microcosms. Samples from all three biological replicates were used for aqueous PFOA quantification, whereas one sequencing profile was generated for each microbial community source–PFOA concentration–sampling day condition. All bottles were incubated in the dark on an orbital shaker at 25 °C and 100 rpm for a total of 75 days. Liquid samples were collected on Days 0, 25, 50, and 75, and aliquots were stored at −20 °C until DNA extraction and PFOA quantification. Day 0 represented the enriched cultures after the three successive transfers and microcosm setup, while the original field communities were not sequenced before enrichment. During the 75-day incubation, dissolved oxygen, pH, residual carbon substrates, nutrient concentrations, microbial biomass, and extracellular polymeric substances (EPS) were not monitored.

2.4. PFOA Analysis

Microbial solutions spiked with PFOA at two levels, along with abiotic controls, were centrifuged at 20,000× *g* for 20 min. The resulting supernatants were collected, diluted with deionized water, and spiked with ^{13}C-PFOA as a non-extracted internal standard to a final concentration of 10 µg/L. PFOA was then quantified on an Agilent 6470 Triple Quadrupole LC–MS/MS system (Agilent Technologies, Santa Clara, CA, USA) in negative electrospray multiple-reaction monitoring (MRM) mode. Aqueous PFOA was quantified in three biological replicate microcosms per treatment condition, and each biological replicate was measured in analytical triplicate by LC–MS/MS. Aqueous PFOA concentrations were calculated relative to the ^{13}C-PFOA internal standard response [64].

2.5. DNA Extraction and 16S rRNA Gene Sequencing and Analysis

A 10-mL aliquot of each culture was centrifuged at 10,000× *g* for 10 min, and the supernatant was discarded to concentrate the biomass into a cell pellet. DNA concentrations in the discarded supernatants were not measured. The sequencing workflow therefore targeted biomass-associated DNA recovered from the pellet, whereas extracellular DNA remaining in the discarded liquid phase was not included. Genomic DNA was extracted from the biomass pellet using the DNeasy PowerSoil Pro Kit (QIAGEN, Hilden, Germany), following the manufacturer's instructions. Environmental DNA comprises both intracellular and extracellular fractions, and the relative contribution of extracellular DNA varies among microbial systems [65,66]. Because DNA in the discarded supernatant was not measured, the sequencing profiles represent pellet-associated bacterial DNA rather than the complete intracellular-plus-extracellular DNA pool. DNA concentrations were quantified on a Qubit 3.0 fluorometer (Thermo Fisher Scientific, Waltham, MA, USA) prior to library preparation. The sequencing libraries were prepared using the 2 × 250 bp kit. The targeted V3–V4 regions of 16S rRNA genes were amplified using the following primers: 16S 341F (5′-CCTACGGGNGGCWGCAG-3′) and 16S 785R (5′-GACTACHVGGGTATCTAATCC-3′). After barcoding and indexing, the library was circularized and sequenced on the Illumina platform. The Bases2Fastq software (v1.4.0; Element Biosciences, San Diego, CA, USA) was used to convert the bases files into FASTQ files and de-multiplex the pooled library based

on index sequences. Data processing was performed following the established Mothur protocol (software version 1.48.2) [67,68]. After removal of barcodes, primer sequences, low-quality reads, and chimeras, the remaining amplicon reads were rarefied to the minimum sequencing depth across samples to minimize biases associated with uneven coverage [69]. Operational taxonomic units (OTUs) were generated at a 97% sequence identity threshold and taxonomically classified against the SILVA reference database (Release 138.2), and the same rarefied OTU table was used as input for both the diversity and Tax4Fun2 functional prediction analyses to ensure internal consistency.

2.6. Microbial Function Prediction

Putative functional traits of each sample were predicted using the Tax4Fun2 R package [70] by analyzing enzyme genes and metabolic pathways based on microbial profiles with taxonomic information. Briefly, the representative sequence of each OTU was queried against the KEGG (Kyoto Encyclopedia of Genes and Genomes) database, in which functional profiles are linked to genome-level taxonomic keys, using a uclust identity threshold of 100% ("Ref100NR" mode). The OTU abundance table from the final step of the Mothur pipeline (97% identity threshold, species level) was then used to map functional profiles to each OTU [71]. Tax4Fun2 outputs comprised relative abundance tables of KEGG level 3 pathways and individual enzymes (EC numbers), which were used for the downstream functional analyses.

2.7. Bacterial Community Assembly Mechanism

Community assembly mechanisms were further evaluated using the beta-nearest taxon index (βNTI), which partitions the relative contributions of stochastic and deterministic processes in community turnover. These processes are partitioned into five categories: heterogeneous selection, homogeneous selection, homogenizing dispersal, dispersal limitation, and drift (including other undetermined processes) [72]. Within this framework, a value of $|\beta NTI| > 2$ indicates that deterministic processes dominate community turnover, with $\beta NTI > +2$ reflecting heterogeneous selection (different environmental filters selecting for different phylogenetic clades) and $\beta NTI < -2$ reflecting homogeneous selection (similar filters selecting for similar clades). Moreover, $|\beta NTI| \leq 2$ reveals the dominance of stochastic processes, indicating that the turnover of the bacterial community is governed by dispersal limitation, homogenizing dispersal, or other undetermined processes. To further evaluate the importance of stochastic processes, a neutral community model (NCM) was fitted to relate the detection frequency of each OTU to its mean relative abundance across the broader metacommunity [73]. In general, the model predicts that taxa that are abundant in the metacommunity will be widespread, since they are more likely to disperse by chance among different sampling sites. In contrast, rare taxa are more likely to be lost in different sites due to ecological drift (i.e., the stochastic loss and replacement of individuals) [74]. Hmisc (version 5.0.1), minpack.lm (version 1.2.3), and getopt (version 1.20.3) packages in R were used for the NCM.

2.8. Statistical Analysis

Temporal compositional stability was quantified using the average variation degree (AVD) following Xun et al. (2021) [59]. For genus i in sample j, the standardized variation degree was calculated as:

$$a_{ij} = \frac{\left| x_{ij} - \overline{x}_i \right|}{\delta_i}$$

where x_{ij} is the relative abundance of genus i in sample j, $\overline{x}_i$ is its mean relative abundance across the samples included in the same microbiome–PFOA treatment group, and δ_i is the corresponding standard deviation. The community-level AVD was then calculated as:

$$\text{AVD} = \frac{1}{kn}\sum_{j=1}^{k}\sum_{i=1}^{n} a_{ij}$$

where k is the number of samples in the treatment group, and n is the number of genera. AVD therefore represents the mean standardized deviation of genus-level relative abundances from their group means. Lower AVD values indicate smaller community-wide compositional fluctuations and greater temporal compositional stability, whereas higher values indicate greater temporal turnover. In this study, stability refers specifically to compositional constancy during the post-enrichment incubation period and excludes functional stability, resistance, or recovery following disturbance.

Principal coordinate analysis (PCoA) was performed to compare community similarity based on weighted UniFrac distances computed from the rarefied OTU table [75], using the phyloseq R package [76]. Linear discriminant analysis (LDA) effect size (LEfSe) was used to identify taxa most likely to explain differences among groups (PFOA concentrations or sampling days), based on the non-parametric factorial Kruskal–Wallis sum-rank test followed by the (unpaired) Wilcoxon rank-sum test [77]. The determining taxon was defined as the representative biomarker of the specific group [78]. For each sequencing-derived alpha diversity metric (Sobs, Shannon, Simpson, ACE, Chao1, and Good's coverage), an exploratory additive linear mixed-effects model was fitted to observations from Days 25, 50, and 75. Microbial community source, PFOA concentration, and sampling day were included as fixed effects. A random intercept was included for each of the six source–concentration series to account for repeated observations over time. Day 0 was excluded because it represented a source-specific background measured before assignment to the PFOA treatments. Given the limited number of sequencing profiles and the absence of within-condition sequencing replication, the models were restricted to additive main effects and excluded interaction terms. Overall fixed effects were evaluated using likelihood-ratio tests. Fixed-effect estimates were standardized by the observed standard deviation of each diversity metric to permit comparison among metrics. Because the estimated random intercept variance approached zero, the model estimates and nominal p-values were interpreted as exploratory. One-way ANOVA followed by the Tukey–Kramer post-hoc test was applied across comparable samples to evaluate the statistical significance of differences in taxon abundances and predicted functional pathways. The p-values from the multiple ANOSIM and Kruskal–Wallis comparisons were adjusted for the false discovery rate (Benjamini–Hochberg). All statistical analyses were performed in R with significance reported at $\alpha = 0.05$ unless otherwise stated.

3. Results

3.1. Decrease in Aqueous PFOA

Aqueous PFOA concentrations were monitored under the two spiking levels (1 and 10 mg/L) over the 75-day incubation in both enriched consortia and in autoclaved abiotic controls (Figure 1). A modest decrease in aqueous PFOA concentration was observed only at the 1 mg/L exposure level, whereas no clear decreasing trend relative to Day 0 was observed at 10 mg/L in either microbial treatment. At Day 75 under the 1 mg/L treatment, freshwater-derived consortia achieved a marginally higher reduction in aqueous PFOA (≈13%) than salt-marsh-derived consortia (≈11%) relative to their respective Day 0 values, while abiotic controls showed no comparable decrease. Because transformation products and fluoride release were not measured, this decrease should not be interpreted as evidence of PFOA

biodegradation. In contrast, abiotic controls retained 95–100% of their initial aqueous PFOA across the 75-day incubation at both concentrations, indicating that biomass-associated processes may have contributed to the modest aqueous PFOA decrease observed in biotic treatments. At Day 25, the mean aqueous PFOA concentration in some biotic treatments was slightly higher than the corresponding Day 0 value. No statistical comparison was performed specifically between Day 0 and Day 25, and therefore, this apparent increase should not be interpreted as statistically significant. The available measurements were unable to distinguish technical variation arising from sample preparation and LC–MS/MS analysis from redistribution of PFOA between the aqueous and biomass-associated phases.

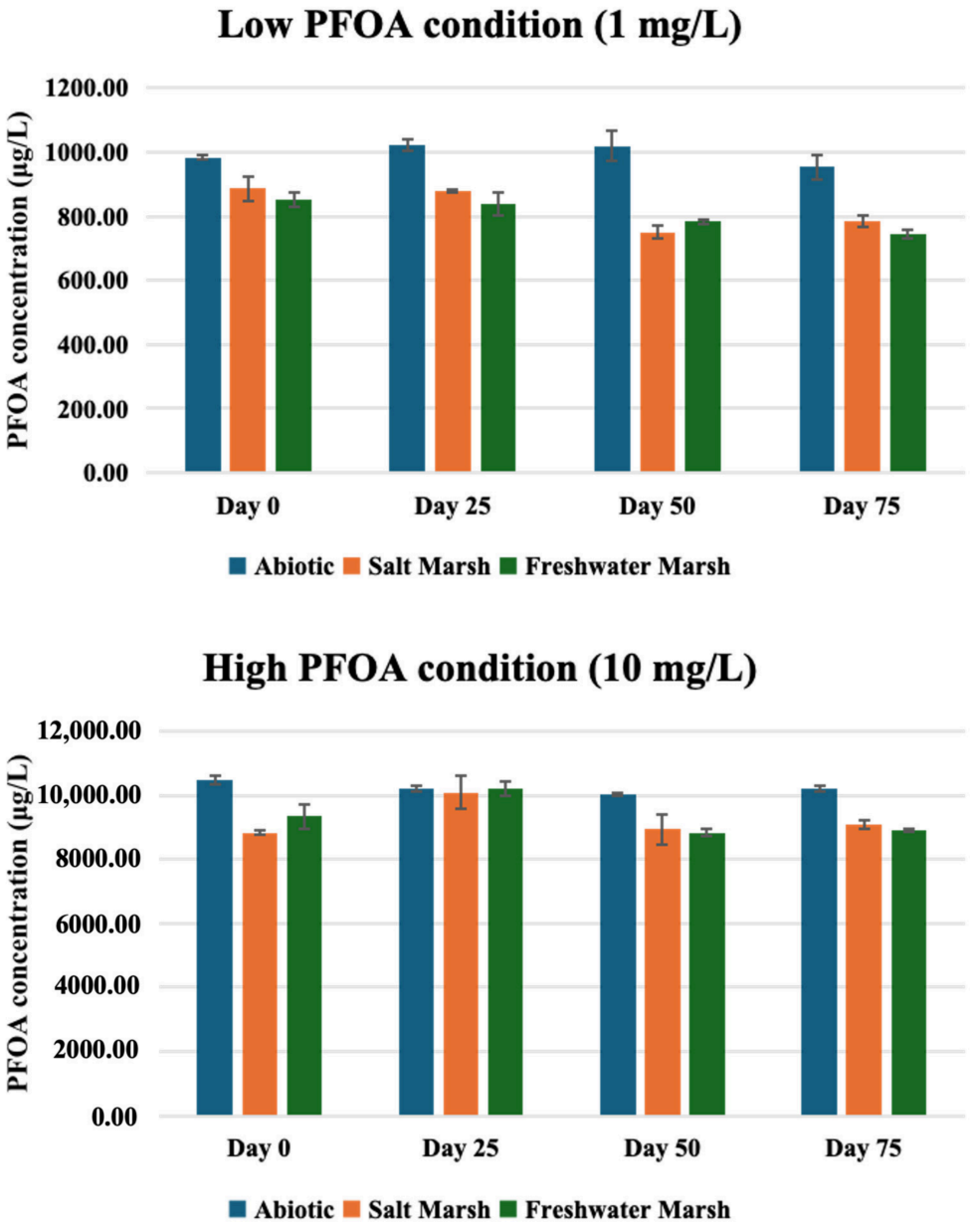


Figure 1. Decrease in aqueous PFOA by freshwater and salt-marsh-derived consortia over a 75-day microcosm incubation. Aqueous-phase PFOA concentrations are shown in the (**top**) low-PFOA treatment (1 mg/L) and (**bottom**) high-PFOA treatment (10 mg/L) for the freshwater marsh, salt marsh, and autoclaved abiotic controls at Day 0, 25, 50, and 75. Data are presented as the mean ± standard deviation of three biological replicates (n = 3); each biological replicate was measured in analytical triplicate by LC–MS/MS.

3.2. Microbial Community Structures

3.2.1. Microbial Diversity

At Day 0, the freshwater-derived inoculum exhibited slightly higher richness and diversity (observed species, Sobs = 348; Shannon H′ = 3.34) than the salt-marsh-derived inoculum (Sobs = 307; Shannon H′ = 3.05) (Table S1). In the absence of PFOA (0 mg/L controls), both enriched consortia underwent substantial temporal restructuring. Diversity in both the salt marsh and freshwater marsh controls increased from Day 0 to Day 50, peaking with Shannon indices of 4.42 and 4.55, respectively. By Day 75, however, diversity in both control groups declined, with Shannon indices falling to ~3.2 in both enriched consortia. This suggests that the microcosm incubation conditions themselves induced major structural shifts in both enriched consortia, especially between Day 50 and Day 75. Across the post-enrichment observations from Days 25 to 75, the exploratory additive mixed-effects models indicated nominal overall effects of microbial community source on Sobs ($p < 0.001$), Shannon diversity ($p < 0.001$), Simpson diversity ($p < 0.001$), ACE richness ($p = 0.012$), and Chao richness ($p = 0.009$). In contrast, no nominal overall effect of source was detected on Good's coverage ($p = 0.257$). Sampling day was also associated with Sobs ($p = 0.008$), Shannon diversity ($p < 0.001$), Simpson diversity ($p < 0.001$), ACE richness ($p = 0.006$), and Chao richness ($p = 0.003$), but not with Good's coverage ($p = 0.153$). PFOA concentration showed a nominal overall association only with Shannon diversity ($p = 0.027$), while no nominal overall concentration association was detected for the other alpha diversity metrics ($p \geq 0.104$) (Figure S2A).

For Shannon diversity, the model-estimated marginal means were 4.46 for the freshwater-derived consortium and 3.97 for the salt-marsh-derived consortium. The corresponding marginal means were 4.10, 4.32, and 4.24 at 0, 1, and 10 mg/L PFOA, respectively, and 4.33, 4.51, and 3.81 on Days 25, 50, and 75, respectively (Figure S2B–D). Because the estimated random intercept variance approached zero, these estimates were treated as exploratory and are unable to provide confirmatory evidence of source-dependent PFOA responses.

3.2.2. Microbial Community Stability

The average variation degree (AVD) was used to summarize community-wide temporal fluctuation across all measured time points, as described in Section 2.8. Lower AVD values indicate greater temporal compositional stability, whereas higher values indicate greater temporal turnover. In this analysis, "stability" refers only to temporal variation across the post-enrichment sampling period, while compositional similarity between the enriched cultures and the original field communities was not assessed. Since the measure of stability is over an entire time course, the most direct and standard interpretation comes from the data grouped by PFOA concentration (Figure S3). After the initial adaptation period, the presence of PFOA at either 1 mg/L or 10 mg/L had no significant impact on the overall temporal stability of the salt-marsh-derived consortium compared to the control. All experimental groups displayed similarly elevated AVD values, indicating comparably high temporal turnover. Similarly, PFOA exposure had no effect on the temporal stability of the freshwater-derived consortium, with AVD values comparable across all treatment groups. Therefore, the inherent turnover associated with microcosm incubation dominated the temporal dynamics, but PFOA produced no detectable increase in this turnover. The AVD results suggest that the inherent instability of the laboratory setup was a more powerful influence on community dynamics than the chemical stress from PFOA. Neither community's temporal stability was measurably decreased by the presence of PFOA over the experimental period.

3.2.3. Microbial Community Composition

In both the freshwater- and salt-marsh-derived consortia, incubation time was the strongest factor shaping genus-level community composition (Figure 2A,B). Genus-level community dynamics across PFOA and time showed clear seed-dependent trajectories. The freshwater-derived consortium was broadly dominated by *Pseudomonadota*, *Actinobacteriota*, and *Firmicutes*, with persistent high-abundance taxa such as *Nitrosomonas*, *Bradyrhizobium*, *Simplicispira*, and *Rhodanobacter*. Several genera nonetheless showed time- and dose-associated shifts: *Pseudomonas* peaked early (Day 25) and declined by Days 50–75, whereas taxa such as *Legionella* increased toward later time points (Days 50–75) across treatments, indicating progressive restructuring during incubation rather than a single immediate PFOA shock response. In contrast, the salt-marsh-derived consortium was dominated by marine- and coastal-associated *Pseudomonadota* and *Bacteroidota*, with consistently high signal from *Pseudomonas* and *Hydrogenophaga* across conditions. A pronounced late-stage enrichment of initially low-abundance *Alphaproteobacteria* and *Microbacteriaceae* lineages emerged by Day 75, particularly under PFOA-spiked treatments, suggesting a delayed, dose-amplified selection process. The Circos biplots of the top 5% of genera (Figure 2C,D) confirmed that the same dominant taxa repeatedly formed the compositional backbone of each community across all PFOA conditions over time. The relative share of secondary taxa and the other bacteria fraction varied across sampling days, indicating reweighting within a stable dominant set rather than wholesale turnover. In the salt-marsh-derived consortium, the most pronounced late-stage redistribution occurred among *Rhodobacteraceae*-related lineages by Day 75, consistent with the dose-amplified selection process inferred from the heatmap.

3.2.4. Microbial Community Similarity

Principal coordinate analysis (PCoA) on weighted UniFrac distances was used to visualize community-level similarity among samples (Figure 3). Group separation was tested by analysis of similarities (ANOSIM), reporting the R statistic and associated *p*-value. PCoA ordination revealed that incubation time was the dominant driver of beta diversity, whereas PFOA concentration (0, 1, 10 mg/L) produced no detectable compositional separation in either seed microbiome. In the freshwater-derived consortium, samples showed no separation by PFOA dose (ANOSIM $R = -0.2263$, $p = 0.873$) but strong separation by sampling day ($R = 0.9753$, $p = 0.001$). The day-grouped ordination was dominated by PC1 (71.29%) and PC2 (13.82%), consistent with a pronounced temporal trajectory across the 75-day incubation. The salt-marsh-derived consortium showed the same pattern that no separation by PFOA concentration ($R = -0.2510$, $p = 0.855$) but clear grouping by day ($R = 0.9095$, $p = 0.001$), with the ordination dominated by PC1 (77.03%) and PC2 (17.22%) in the day-grouped plot. The large fraction of variance captured along PC1 (>70%) in both enriched consortia, together with sampling order, is consistent with a directional, succession-like trajectory, motivating the null-model analyses (Section 3.3).

A supervised partial least squares discriminant analysis (PLS-DA) was applied to identify genus-level features that best separated the predefined PFOA treatment groups (Figure S4). PLS-DA revealed a distinct separation between the control group (0 mg/L) and the two PFOA-treated groups (1 and 10 mg/L). This separation occurred primarily along the COMP1 axis, which explains 13.13% of the variance. All control samples had negative values on the COMP1 axis, while nearly all PFOA-exposed samples had positive values. The 1 mg/L (light blue triangles) and 10 mg/L (dark green diamonds) groups largely overlapped with each other on the right side of the plot. No clear separation was observed between the two PFOA concentrations, indicating that the genus-level signature of PFOA exposure was qualitatively similar across the two doses tested.

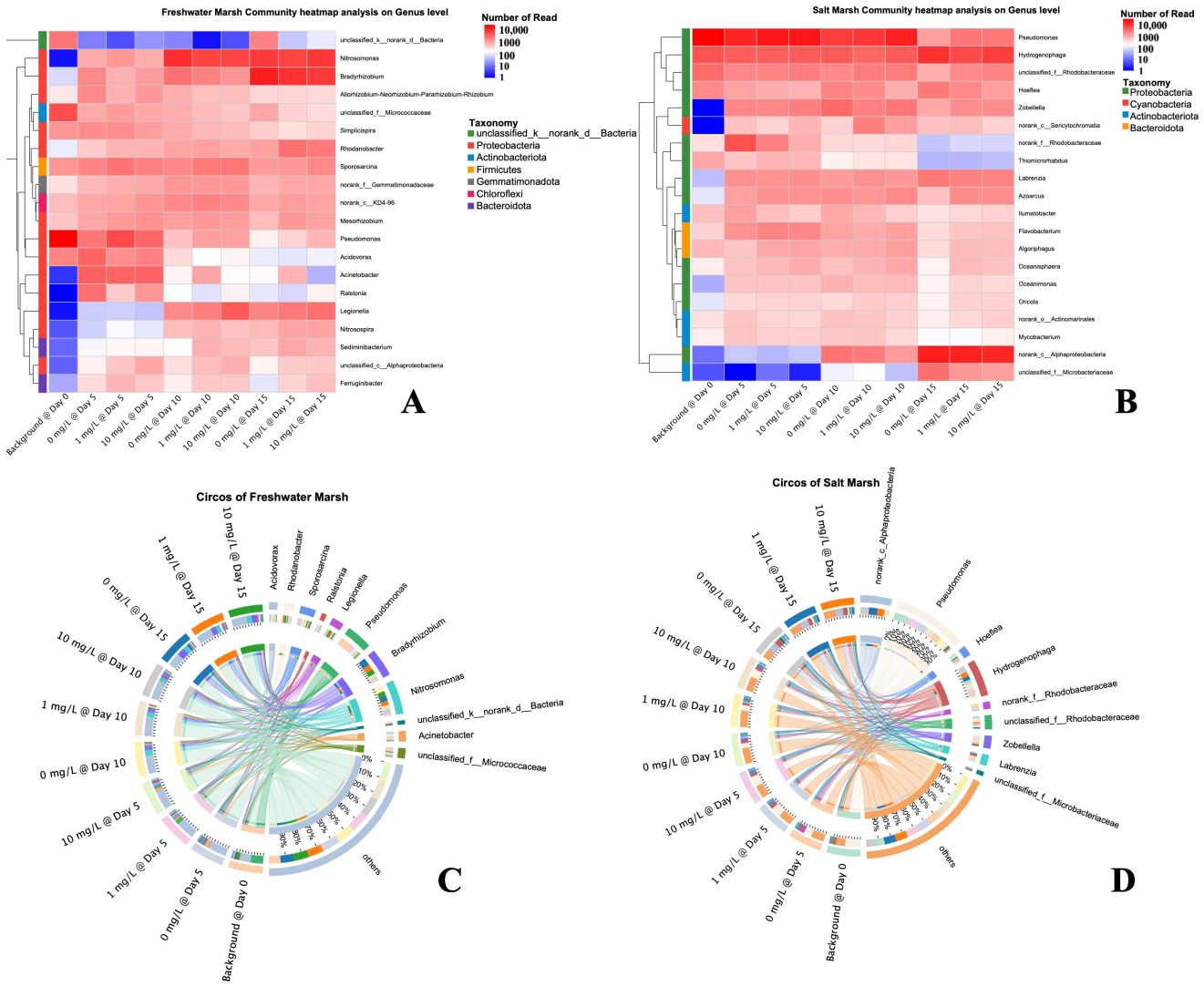


Figure 2. Temporal and compositional dynamics of microbial communities under PFOA exposure. Genus-level relative abundance heatmaps across all sampling days (Day 0, 25, 50, 75) and PFOA concentrations (0, 1, 10 mg/L) for the (**A**) freshwater-marsh-derived and (**B**) salt-marsh-derived consortia. Circos biplots displaying the proportional contribution of the top 5% dominant genera across all treatment conditions and sampling days for the (**C**) freshwater-marsh-derived and (**D**) salt-marsh-derived consortia.

3.3. Microbial Ecology and Interaction

3.3.1. Community Assembly Process

To partition the relative contributions of deterministic and stochastic processes to community assembly, a phylogenetic null-model framework based on the beta-nearest taxon index (βNTI) was applied (Figure 4). In both enriched consortia (Figure 4B,C), Day 50 and Day 75 turnover was attributed almost entirely to drift and other undetermined processes (~1.0), indicating that incubation-driven succession became overwhelmingly stochastic at the later stages of the experiment. At Day 0, both enriched consortia showed substantial heterogeneous selection (~0.45) and an additional dispersal limitation component (~0.20–0.25), with drift accounting for the remainder, indicating strong initial niche differentiation and dispersal constraint in the starting inocula. When summarized by PFOA concentration (Figure 4A), the freshwater-derived consortium remained largely drift-dominated at 0 and 1 mg/L (with smaller contributions from heterogeneous selection and dispersal limitation), whereas at 10 mg/L drift increased further, with dispersal limitation persisting as the

primary non-drift component. In contrast, the salt-marsh-derived consortium exhibited a dose-amplified deterministic signature. Heterogeneous selection became the dominant process at 1 mg/L and remained substantial at 10 mg/L, indicating that PFOA imposed markedly stronger niche-based filtering on the salt-marsh-derived consortium than on the freshwater-marsh-derived consortium under the same exposure regime. Overall, incubation time drove both enriched consortia toward stochastic assembly, but PFOA imposed a comparatively stronger, seed-dependent deterministic signature on the salt-marsh-derived consortium, consistent with greater sensitivity of its phylogenetic turnover to PFAS stress. These assembly patterns differed between the two enriched consortia, however, they should not be interpreted as confirmation of source-dependent PFOA effects on alpha diversity because source × PFOA interactions could not be evaluated in the alpha diversity analysis.

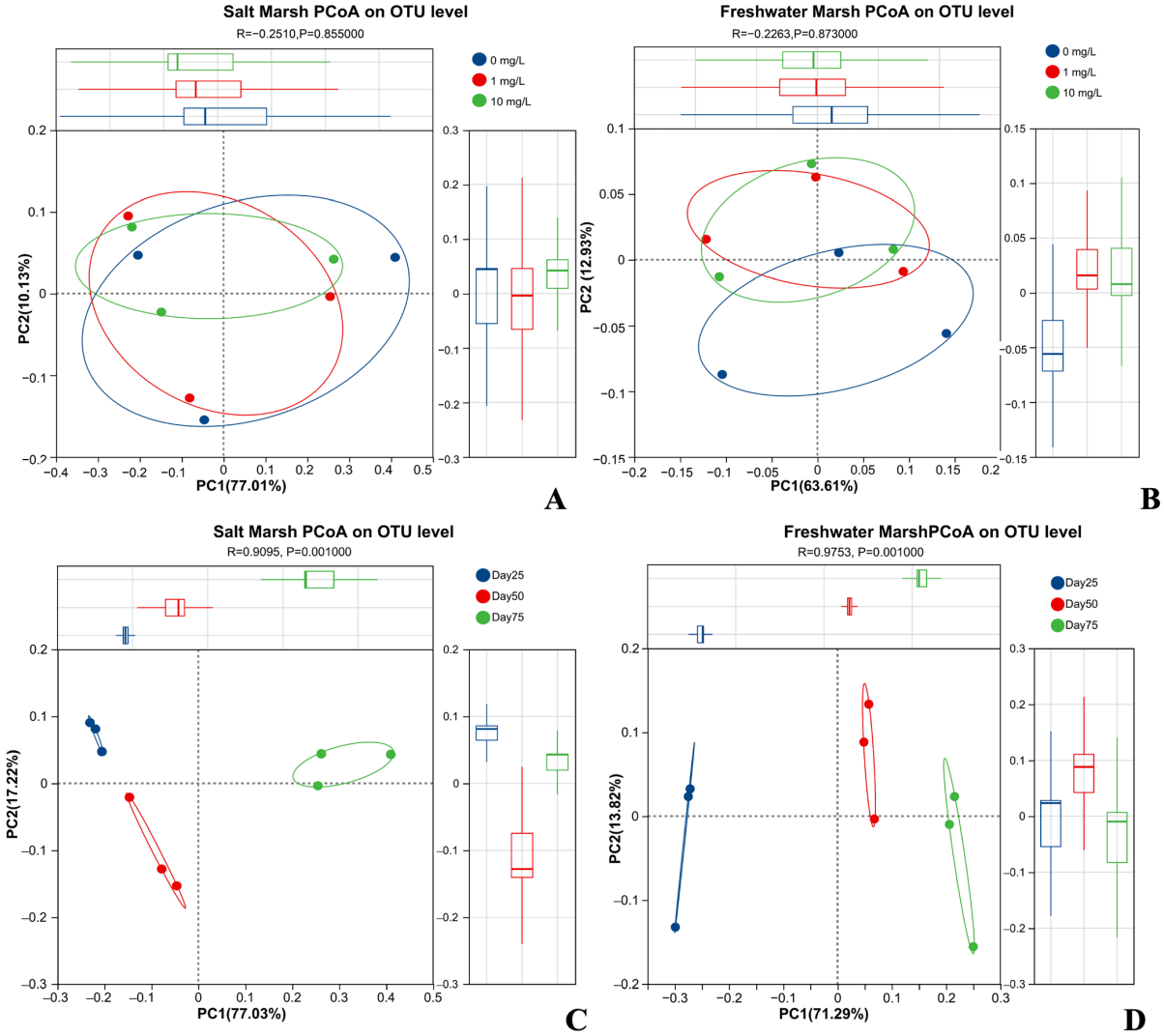


Figure 3. Principal coordinate analysis (PCoA) of microbial beta diversity based on weighted UniFrac distances. Samples from the salt-marsh-derived consortium grouped by (**A**) PFOA concentration and (**C**) sampling day; samples from the freshwater-derived consortium grouped by (**B**) PFOA concentration and (**D**) sampling day. Variance explained by each principal coordinate (PC1, PC2) and the corresponding ANOSIM R and *p*-values are reported on each panel. Note that PFOA concentration groupings yielded ANOSIM R values near zero in both enriched consortia ($p > 0.85$), whereas sampling day groupings yielded $R > 0.90$ ($p = 0.001$), indicating that incubation time was by far the dominant axis of beta-diversity variation.

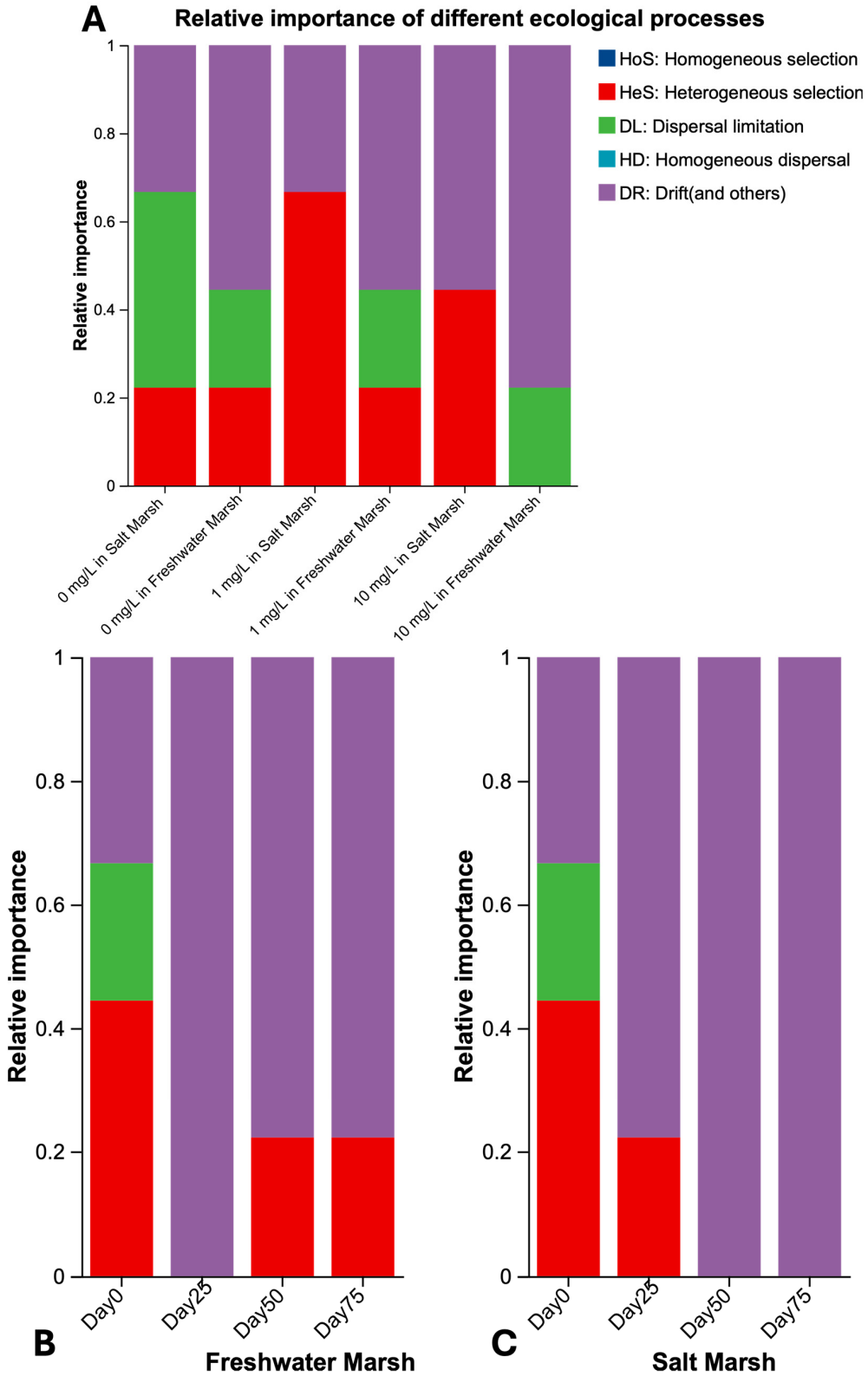


Figure 4. Ecological assembly processes governing microbial community turnover, assessed using the beta-nearest taxon index (βNTI). Relative contributions of stochastic and deterministic processes (heterogeneous selection, homogeneous selection, dispersal limitation, homogenizing dispersal, and drift/others) are summarized by (**A**) PFOA concentration, shown separately for the salt-marsh-derived and freshwater-derived consortia and pooled across sampling days, (**B**) sampling time point in the freshwater-derived consortium, and (**C**) sampling time point in the salt-marsh-derived consortium.

3.3.2. Neutral Community Model

The neutral community model (NCM) developed by Sloan et al. quantifies the fraction of community structure that can be explained by stochastic dispersal and ecological drift in microbial systems [73]. When each seed microbiome was modeled independently, the NCM explained a large fraction of the occurrence–abundance relationship (R^2 = 0.87 for the freshwater-derived consortium, and R^2 = 0.89 for the salt-marsh-derived consortium; Figure 5A,B). However, this neutral fit collapsed when PFOA-exposed samples (1 and 10 mg/L) were pooled across both seed microbiomes (R^2 = −0.85; Figure 5C). The migration rate (m) was higher in the freshwater-derived consortium (m = 1.13) than in the salt-marsh-derived consortium (m = 0.85), indicating weaker dispersal limitation and more efficient exchange of taxa between the metacommunity and local microcosms in the freshwater system. A larger fraction of OTUs in the salt-marsh-derived consortium fell below the 95% confidence interval of the neutral prediction, indicating that more taxa are under environmental filtering or selective pressure, consistent with the lower m value. The effective dispersal parameter (Nm) quantifies the strength of dispersal from the metacommunity to the local communities. The higher Nm of the freshwater-derived consortium is consistent with a more open assemblage with greater microbial exchange, whereas the salt-marsh-derived consortium experienced stronger dispersal filtering. The lower migration rate and stronger dispersal limitation of the salt-marsh-derived community indicate a source-associated difference in community assembly. Salinity and osmotic stress can affect microbial dispersal and assembly in saline environments.

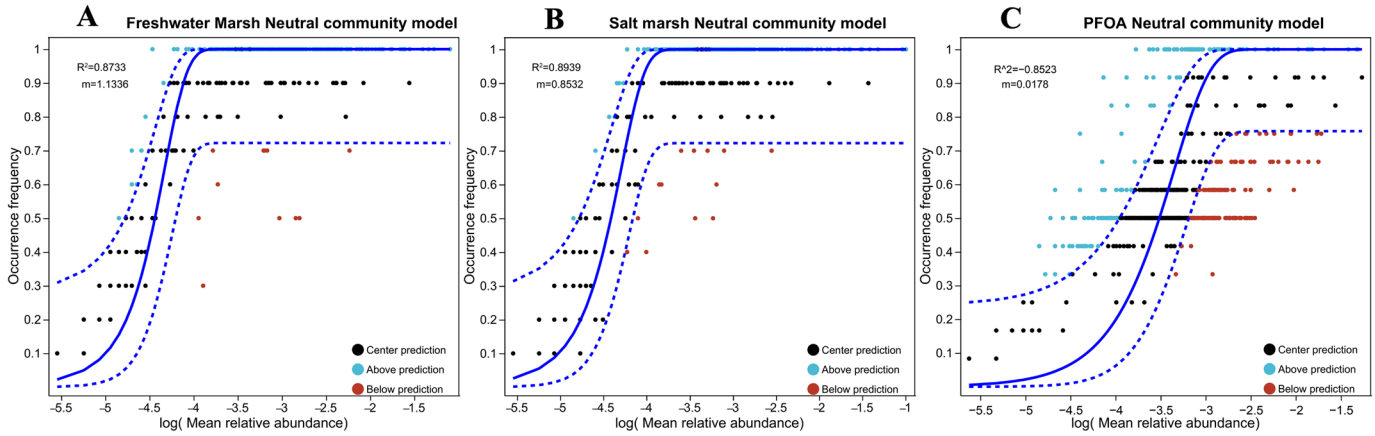


Figure 5. Neutral community model (NCM) fitting of microbial community occurrence–abundance relationships. NCM curves were fitted independently to (**A**) freshwater-derived consortia and (**B**) salt-marsh-derived consortia, with OTUs above (cyan) and below (red) the 95% confidence interval highlighted. The solid blue line represents the NCM-predicted occurrence frequency, and the dashed blue lines indicate the corresponding 95% confidence interval. (**C**) NCM applied to PFOA-exposed communities (1 and 10 mg/L) pooled across both seed microbiomes and all sampling days. Migration rate (m), effective dispersal (Nm), and model fit (R^2) are reported for each condition. Model fit (R^2) and m values are shown in each panel. N = 35,086 for all three models, and Nm values were 39,775.0677 for the freshwater marsh (**A**), 29,935.0375 for the salt marsh (**B**), and 625.4276 for the pooled PFOA-exposed communities (**C**).

3.3.3. Potential Biomarker Taxa Identification

To identify potential microbial biomarkers of PFOA exposure, the non-parametric Kruskal–Wallis H test was applied across PFOA concentrations after pooling samples regardless of sampling day (Figure 6A,D). In the salt-marsh-derived consortium, OTU98 (*Pseudohongiella*), OTU304 (*Flavobacterium*), OTU439 and OTU428 (*Parvibaculum*), OTU66 (*Edaphobaculum*), and OTU65 (uncultured *KD4-96*) showed their highest relative abundance

in the control (0 mg/L) and decreased in the presence of PFOA. These taxa are therefore candidate PFOA-sensitive lineages in this enriched consortium, whereas no genus was significantly enriched at 10 mg/L PFOA in the salt-marsh-derived consortium. In contrast, OTU627 (uncultured *Sericytochromatia*) in the freshwater-derived consortium showed a clear increase in relative abundance at 10 mg/L, suggesting tolerance to or even a competitive advantage under high-PFOA exposure.

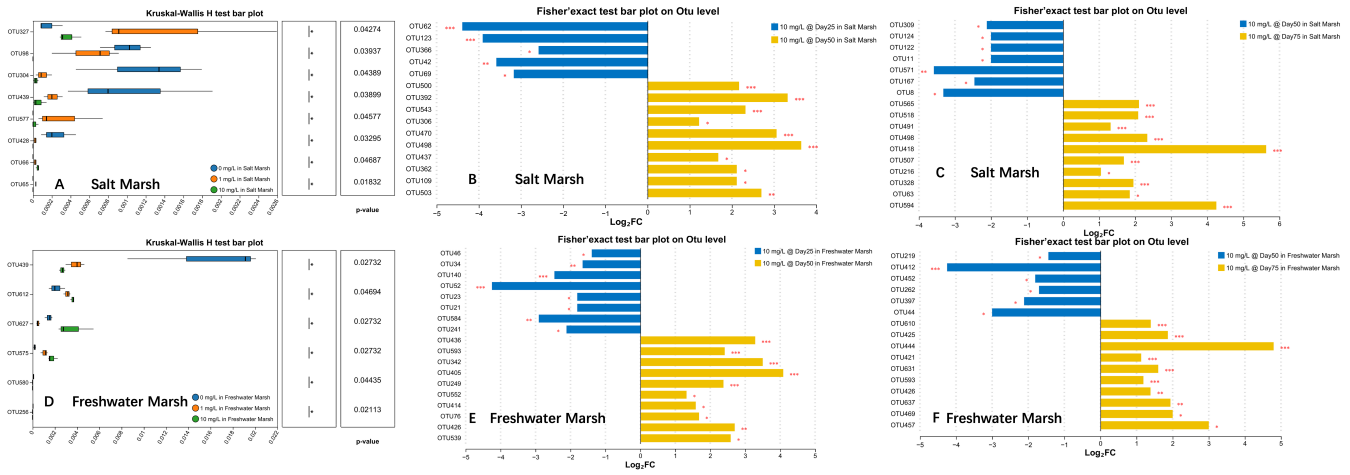


Figure 6. Differential taxa analysis across PFOA treatment groups. (**A**,**D**) Kruskal–Wallis H tests identifying OTUs whose relative abundances differ significantly across PFOA concentrations (0, 1, 10 mg/L) in the salt-marsh-derived consortium and freshwater-derived consortium, respectively, after pooling samples across all sampling days. (**B**,**C**,**E**,**F**) Fisher's exact tests comparing OTU abundances between successive sampling days (Day 25 vs. Day 50; Day 50 vs. Day 75) under 10 mg/L PFOA in each enriched consortium, with significance levels indicated as *** $p < 0.001$, ** $p < 0.01$, * $p < 0.05$. OTUs that are progressively enriched or depleted across these intervals are candidate microbial biomarkers of sustained PFOA exposure in their respective enriched consortia. Panels (**A**–**C**) represent the salt-marsh-derived consortium, whereas panels (**D**–**F**) represent the freshwater-derived consortium.

To further track the temporal emergence of biomarkers, pairwise Fisher's exact tests were used to compare OTU abundances between successive sampling days (Day 25 vs. Day 50; Day 50 vs. Day 75) under 10 mg/L PFOA (Figure 6B,C,E,F). In the salt-marsh-derived consortium, only OTU498 (uncultured Terasakiellaceae) showed a sustained significant enrichment across both intervals. In the freshwater-derived consortium, two *Legionella* OTUs (OTU593 and OTU426) were progressively enriched across both intervals under 10 mg/L PFOA. These progressively enriched lineages are promising candidate microbial biomarkers of sustained PFOA exposure in their respective enriched consortia.

3.4. Predicted Microbial Function

3.4.1. Predicted Pathways

Across all KEGG level 3 pathway predictions, the two seed microbiomes exhibited markedly distinct functional baselines, with smaller within-seed shifts attributable to time or PFOA dose. When comparing salt marsh vs. freshwater marsh (averaged across all timepoints and concentrations, Table S2), the salt-marsh-derived consortium showed higher predicted representation of pathways largely assigned to glycan/lipid-related metabolism and secondary metabolite modules, including fatty acid elongation (ko00062) and multiple glycan biosynthesis pathways (e.g., N-glycan biosynthesis/various N-glycan/O-glycan and glycosphingolipid biosynthesis; ko00513/ko00515/ko00604/ko00510). Predicted representation of flavone/flavonol biosynthesis (ko00944) was also higher. In contrast, the freshwater-derived consortium showed higher predicted representation of several path-

ways annotated under cellular processes/replication–repair and xenobiotic/secondary metabolism, including furfural degradation (ko00365) and multiple terpenoid/polyketide-related modules (e.g., monoterpenoid biosynthesis ko00902; sesquiterpenoid/triterpenoid biosynthesis ko00909), along with DNA-repair-linked functions (e.g., non-homologous end joining ko03450). Together, these predicted profiles indicate greater representation of membrane- and glycan-associated functions in the salt-marsh-derived consortium and of stress response, DNA repair, and xenobiotic transformation functions in the freshwater-marsh-derived consortium under the same incubation design.

ANOVA with Tukey–Kramer post-hoc tests showed that three focal pathways differed primarily by seed microbiome rather than by PFOA dose, with similar patterns for several glycan and secondary metabolite biosynthesis pathways (Figures 7 and S5). Collectively, the predicted potentials for β-lactam-resistance and glutathione-mediated redox buffering were significantly higher in the freshwater-derived consortium, whereas sulfur- and osmolyte-associated metabolism (taurine/hypotaurine) was significantly higher in the salt-marsh-derived consortium. Seed microbiome identity was the dominant driver of the differences in all three pathways, with PFOA concentration producing only smaller, context-dependent modulation of these seed-defined baselines.

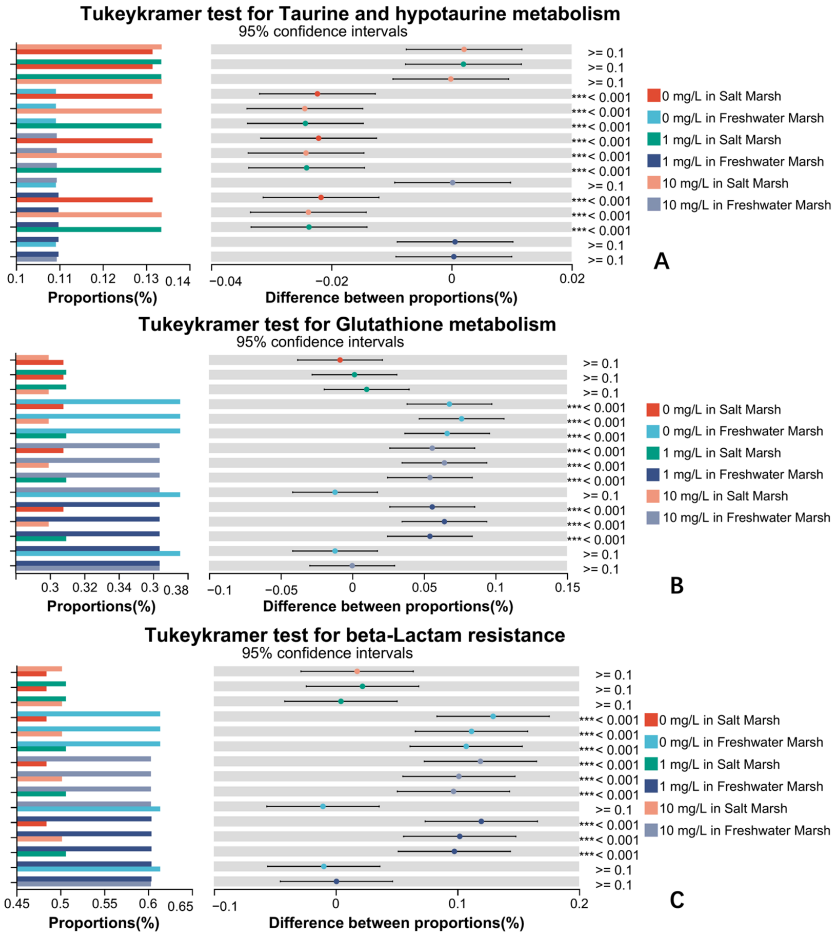


Figure 7. One-way ANOVA with Tukey–Kramer post-hoc comparisons of Tax4Fun2-predicted functional pathway proportions across PFOA concentrations (0, 1, 10 mg/L) and microbiome source (salt marsh vs. freshwater marsh): (**A**) taurine and hypotaurine metabolism (KEGG ko00430), (**B**) glutathione metabolism (ko00480), and (**C**) β-lactam resistance (ko01501). Significant pairwise differences are indicated (*** $p < 0.001$; ** $p < 0.01$; * $p < 0.05$; ns, not significant).

3.4.2. Predicted Enzymes

Across the enzyme prediction tables, the two seed microbiomes showed clear seed-dependent functional baselines, with a subset of enzymes consistently higher in salt marsh versus freshwater marsh (and vice versa) across the full time × PFOA design (Table S3). Salt-marsh-enriched enzymes (Table S3) included redox and carbon–nitrogen-related functions such as lactaldehyde reductase (EC 1.1.1.77), isobutyryl-CoA mutase (EC 5.4.99.13), and guanidinopropionase (EC 3.5.3.17), indicating a stronger predicted capacity for specific aldehyde/CoA transformations and guanidino-compound turnover in the salt-derived community. In contrast, freshwater-derived consortia (Table S3) showed higher predicted representation of multiple oxygenase and xenobiotic-associated enzymes, including limonene 1,2-monooxygenase (EC 1.14.13.107) and phthalate 4,5-dioxygenase (EC 1.14.12.7), consistent with greater predicted potential for oxidative transformation pathways in the freshwater inoculum. Overall, these predicted enzyme-level patterns mirrored the pathway-level results: source microbiome (salt vs. freshwater) explained the dominant functional separation, while time and PFOA were associated with smaller differences in predicted enzyme proportions within that seed-defined backdrop.

Within each seed microbiome, PFOA produced only modest shifts in predicted enzyme profiles over the 75-day incubation, especially when compared with the much larger baseline differences between salt-marsh-derived and freshwater-derived consortia. When restricting to the most abundant enzymes (top quartile by mean abundance), the typical maximum change attributable to PFOA (comparing 1 vs. 0 and 10 vs. 0 mg/L across all sampling days) was small, with median max shifts of ~0.15 log2 in salt marsh and ~0.14 log2 in freshwater (≈10–11% change), and even the extreme abundant-enzyme responses remained limited (99th percentile ~0.63 log2 in salt marsh and ~0.57 log2 in freshwater marsh). The clearest within-seed responses were enzyme-specific and time-dependent: in salt marsh, the largest PFOA-associated shifts among abundant enzymes were observed for xylulokinase (EC 2.7.1.17) and quinone oxidoreductase (EC 1.8.5.4) (strongest at 10 vs. 0 mg/L on Day 25). Asparagine synthase (EC 6.3.5.4) also showed one of the largest shifts (notable at 1 vs. 0 mg/L on Day 75). In freshwater marsh, the strongest abundant-enzyme shifts were concentrated early (Day 25), including mono(ethylene terephthalate) hydrolase (EC 3.1.1.102), aminobutyraldehyde dehydrogenase (EC 1.2.1.19), and phthalate 4,5-dioxygenase (EC 1.14.12.7) (often peaking at 1 vs. 0 mg/L). A smaller late response was observed for ribosome biogenesis GTPase/thiamine phosphatase (EC 3.1.3.100) at 10 vs. 0 mg/L on Day 75. Overall, these patterns suggest that PFOA was not associated with broad changes in predicted enzyme functional potential within either seed over this timescale, and the observed differences were limited to a small subset of enzymes and varied among sampling times.

3.4.3. The Variation of Pathways and Enzymes

The majority of significantly differential predicted enzymes (11 of 16) had consistently higher predicted relative abundance in the salt-marsh-derived consortium than in the freshwater-derived consortium (Figure S6). These salt-marsh-enriched predicted functions were associated with complex macromolecular substrates. In particular, serralysin (EC 3.4.24.40) and creatinase (EC 3.5.3.3) had considerably higher predicted relative abundances in the salt-marsh-derived consortium than in the freshwater-derived consortium, and their predicted proportions tended to increase under PFOA exposure in the salt-marsh-derived consortium (Figure S6). Overall, the predicted enzyme profiles of the two microbial communities were fundamentally distinct. The salt-marsh-derived consortium showed higher predicted representation of enzymes associated with the degradation of complex substrates such as proteins, and this representation tended to increase under PFOA exposure. In

contrast, the freshwater-marsh-derived consortium showed higher predicted representation of a different set of redox and biosynthetic enzymes, several of which also differed across PFOA treatments, indicating contrasting predicted functional profiles between the two source communities. Consistent with the taxonomic shifts (Section 3.2.3) and assembly contrast (Section 3.3), the enzyme-level patterns showed predicted enrichment in extracellular proteolysis and osmolyte-associated functions in the salt-marsh-derived consortium and in oxidative xenobiotic transformation and redox buffering functions in the freshwater-derived consortium. Because dissolved oxygen was not monitored, the contribution of changes in oxygen availability to these predicted functional profiles could not be separated from the PFOA-associated patterns.

4. Discussion

This study examines how the bacterial components of laboratory-enriched microbial consortia derived from freshwater marsh and salt marsh soils responded to PFOA at the levels of taxonomy, community assembly, and predicted function. Serial cultivation can select microorganisms suited to the supplied growth conditions and alter community composition [58]. These cultures were generated through a top-down enrichment procedure using natural environmental inocula and therefore differ from synthetic communities assembled from selected isolates. Nevertheless, cultivation in defined media and serial transfer may impose strong selection. The resulting consortia should not be treated as intact representations of the source wetland microbiomes. Even so, this design followed previous enrichment-based work, where natural soil inocula were grown and serially transferred in defined media to yield tractable consortia for controlled experiments. The inoculum preparation procedure introduced an additional source of selection because pyrophosphate dispersion, low-speed centrifugation, and 70-µm straining preferentially recovered suspended and loosely particle-associated bacteria, while tightly particle-associated cells and larger fungal structures may have been depleted [48,49]. These consortia retained taxa and compositional features associated with their source soils, but cultivation and serial transfer selected a reduced subset of the original communities and progressively washed out some low-abundance taxa [55,56]. Because low-abundance taxa can make disproportionate contributions to microbial community function, the taxa lost during enrichment may contain ecologically important organisms, including potential contributors to PFOA transformation. The findings therefore describe responses of enriched cultures but not the in-situ wetland microbiomes. Supplying the carbon mixture as a proxy for the organic carbon associated with soil TOC was intended to sustain microbial growth and to avoid community changes associated with carbon deprivation [62,63]. Direct exposure experiments using unmanipulated field communities would be needed to determine whether the observed responses also occur within native wetland matrices. Because dissolved oxygen, pH, residual carbon substrates, nutrient concentrations, microbial biomass, and EPS were not monitored during incubation, their potential contributions to microbial community dynamics and PFOA adsorption could not be evaluated, and a complete PFOA mass balance could not be established. The sequencing profiles represent DNA recovered from the centrifuged biomass pellets. Because DNA in the discarded supernatants was not measured, the contribution of extracellular DNA released into the liquid phase could not be quantified. The carbon mixture was supplied as the carbon source, and carbon-mixture-free controls were not included. The independent contribution of carbon-supported growth to the observed taxonomic and diversity patterns therefore could not be separated from the effects of PFOA exposure.

Moreover, the salt-marsh-derived cultures were maintained in marine AMS containing 20 g/L NaCl, whereas the freshwater-marsh-derived cultures were maintained in AMS

without added NaCl. The experimental design is therefore unable to separate the effect of microbiome source from that of culture salinity. Accordingly, the observed differences are interpreted as contrasts between the two source-derived consortia under their respective culture conditions. The contributions of prior PFOA exposure and specific site environmental factors to the community differences and PFOA responses cannot be resolved from the available data. Multicountry monitoring studies illustrate the variability of PFOA concentrations in surface waters. Baabish et al. (2021) quantified PFOA at 0.05–4.02 ng/L in 144 surface water samples from 22 countries, while Kunacheva et al. (2012) reported city-average river water concentrations of 0.2–1630.2 ng/L across 41 cities in 15 countries, with higher concentrations in industrialized areas [54,79]. For regulatory context, the U.S. Environmental Protection Agency established an enforceable maximum contaminant level of 4.0 ng/L for PFOA in drinking water (U.S. EPA, 2024) [80]. Although this standard applies to drinking water rather than wetland soil or surface water, it further illustrates the substantial difference between regulatory-scale concentrations and the 1–10 mg/L treatments used in this study. A point worth addressing explicitly is the gap between the PFOA concentrations used here (1 and 10 mg/L) and the ng/L–µg/L levels typical of background coastal surface waters. The deliberate use of elevated doses in microcosm experiments is, however, an approach used in PFAS microbial ecology studies [60,61] for several reasons. PFOA-induced microbial growth inhibition and cellular stress have been documented in laboratory experiments [81]. First, microbial community responses, such as taxonomic reshuffling, assembly regime shifts, and predicted functional re-allocation, can be examined under elevated PFOA exposure alongside the strong incubation-driven succession signal documented here (Sections 3.2 and 3.3). Previous freshwater community experiments have examined responses at 5 and 10 mg/L PFOA [60,61], while the exposure duration needed to generate comparable community-level signatures at ng/L concentrations was not assessed in the present study. Second, microbial communities at the sediment-water interface and in EPS-rich biofilms may encounter PFOA associated with the biofilm matrix, as PFOA binding to sludge EPS proteins has been characterized, and PFOA has been measured in natural river biofilms at 463.73 ± 601.16 ng/g wet weight (n = 3) [82,83]. These processes provide a mechanistic context for microbial exposure, although a 1–10 mg/L aqueous treatment in the present microcosms cannot be directly equated with local microbe-scale exposure under chronic, lower aqueous contamination. Finally, the two doses (1 vs. 10 mg/L) provide a 10-fold exposure contrast. At 1 mg/L, the observed decrease in aqueous PFOA was consistent with a possible contribution from biosorption; the same pattern was not detected at 10 mg/L. This concentration-dependent difference provides a basis for comparing microbial responses between the two treatments. The magnitudes and directions of the responses observed at 1 and 10 mg/L are specific to the enriched consortia and the tested culture conditions and should not be extrapolated to chronic field exposure at ng/L–µg/L concentrations. Analytical resolution was an additional practical consideration in selecting elevated exposure concentrations. At ng/L exposure levels, small temporal changes in aqueous PFOA could be comparable to the sampling and analytical variability of the present experimental design, whereas the mg/L treatments provided a concentration contrast that could be resolved more reliably.

Both enriched consortia attenuated aqueous PFOA concentrations only modestly, with a measurable decrease restricted to the lower 1 mg/L exposure and no detectable reduction at 10 mg/L. Both the magnitude and the concentration dependence of these dynamics are consistent with potential biosorption-dominated immobilization, possibly involving association of PFOA with the extracellular polymeric substances (EPS) matrix and adsorption to microbial cell surfaces [84]. Prior work observed increased secretion of tryptophan-like and humic-like fluorescent components in response to PFOA, consistent with the active produc-

tion of EPS as a protective barrier that fortuitously immobilized the toxicant [84]. Consistent with this possible explanation, microalgal-mediated bioremediation by *Scenedesmus quadricauda* was shown to remove 44.8% of PFOA via bioaccumulation and 12.8% via bioabsorption, with only 0.58% biodegraded after 30 days [85]. The small magnitude of the difference in removal between the two source-derived consortia is consistent with a possible role for physicochemical partitioning in the observed aqueous PFOA attenuation. Under high-salinity conditions, divalent cations and elevated ionic strength promote partitioning of PFOA onto the solid phase. This partitioning may dampen aqueous PFOA exposure and the resulting selective pressure on microbial populations [86]. If PFOA loss were driven by passive equilibrium partitioning to biomass, removal would depend on the available sorbent surface and the partitioning behavior at each loading. The absence of a measurable decrease at 10 mg/L may reflect PFOA suppression of the active biomass and EPS production involved in immobilization, consistent with prior reports that elevated PFOA compromises membrane integrity and reduces bacterial viability [81]. The observed values describe a decrease in aqueous PFOA concentration, with biosorption and phase partitioning considered possible contributing processes. Phase-resolved PFOA measurements, transformation product analysis, and fluoride release measurements would be needed to evaluate these processes [87].

The exploratory alpha diversity analysis indicated that microbial community source and sampling day were the principal correlates of richness and diversity, whereas PFOA concentration showed a nominal overall association only with Shannon diversity. The model-estimated Shannon mean was lower for the salt-marsh-derived consortium than for the freshwater-derived consortium and varied across the post-enrichment sampling days. Because interaction terms were not included in the additive models, the apparent source-specific concentration patterns cannot establish that PFOA increased diversity in one consortium while suppressing it in the other. Salinity and tidal variability can impose osmotic stress on salt marsh microbial communities. Such background constraints may increase sensitivity to an additional stressor such as PFOA, although their contribution could not be evaluated without site-specific physicochemical measurements [88]. This is consistent with the decline of marine-associated genera such as *Pseudohongiella* and *Flavobacterium* in the salt-marsh-derived consortium under PFOA exposure, leaving a simplified community dominated by a smaller set of specialized and tolerant taxa. Within the tested enriched consortia, the contrasting diversity responses were associated with microbiome source and culture conditions. Their relevance to the stress tolerance of native wetland communities remains unresolved. In addition, carbon substrates and the different AMS formulations may also have contributed to the observed diversity patterns through cultivation-related selection. Because carbon-free controls were not included, the contributions of carbon supplementation, culture salinity, and PFOA exposure cannot be separated in the present design.

The source-specific patterns observed in the unadjusted Shannon profiles may be consistent with a competitive-release mechanism, although this interpretation remains hypothetical because source × PFOA interactions could not be tested in the present design. In the freshwater-derived consortium, the incubation-driven decline of dominant *Pseudomonadota*, exemplified by the time-dominant *Pseudomonas* lineage, may have opened niche space that was further modified under PFOA exposure. That niche space may have allowed previously rare but tolerant lineages to expand, such as the OTU627 *Sericytochromatia* genotype identified as a candidate PFOA-associated taxon in the freshwater-derived consortium (Figure 6). The community thus appeared more diverse under PFOA, possibly not because growth was stimulated in absolute terms, but because PFOA-tolerant rare lineages may have been able to fill the niches opened by incubation-driven succession. In

the salt-marsh-derived community, the baseline composition may have been shaped by both the source environment and the saline culture medium. PFOA-associated declines in sensitive marine-associated taxa (*Pseudohongiella*, *Flavobacterium*, *Parvibaculum*) may have contributed to the observed decrease in Shannon diversity. This possible competitive-release interpretation is qualitatively consistent with the assembly evidence that the freshwater-derived consortium remained drift-dominated under PFOA, signaling sustained stochastic replacement of disturbed positions, whereas the salt-marsh-derived consortium shifted into heterogeneous, niche-based selection, indicating that only a subset of pre-adapted genotypes could occupy the post-disturbance space.

The intrinsic temporal trajectory of microcosm incubation, driven by nutrient drawdown and competition, can produce a strong temporal signal that overshadows more subtle contaminant-driven effects on beta diversity [89,90]. The present finding that incubation time was a far stronger driver of beta diversity than PFOA concentration aligns with these observations and reinforces the value of time-resolved sampling for distinguishing incubation-driven succession from PFOA-associated changes [91]. PFOA can inhibit microbial growth under laboratory exposure conditions [61], but the present data are insufficient to establish that biomass inhibition caused the absence of detectable aqueous PFOA attenuation at 10 mg/L. Although some microbial consortia can transform or partially defluorinate PFOA, this capacity is typically restricted to narrow physicochemical windows and concentrations [87,92,93]. The abundances of *Pseudohongiella*, *Flavobacterium*, and *Parvibaculum* declined in the salt-marsh-derived consortium under the tested PFOA treatments. Conversely, *Pseudomonas* persisted in both source-derived consortia despite frequently occurring below the neutral-model prediction. This persistence is consistent with the metabolic versatility of this genus and its documented role in xenobiotic catabolism [94–97]. The selective enrichment of *Sericytochromatia* in the freshwater-derived consortium at 10 mg/L PFOA is of particular ecological interest. As a non-photosynthetic sister lineage of cyanobacteria, *Sericytochromatia* carries genomic signatures of oxidative stress tolerance that may, speculatively, also confer tolerance to PFOA-induced membrane and redox stress [98]. Taken together, these taxonomic shifts indicate source-dependent responses to PFOA in the two enriched consortia. The potential sensitivity of nitrogen-fixing genera such as *Bradyrhizobium* under PFAS stress also deserves attention. Because nitrogen cycling activity was not measured, the present study cannot determine whether these taxonomic responses affected biological nitrogen input or primary productivity [99–101]. *Legionella* and *Pseudomonas* are known to thrive in biofilms and can enhance the thickness and rigidity of the biofilm matrix, and PFOA has been shown to stimulate biofilm density and extracellular polysaccharide production that creates a protective physical defense mechanism [102,103].

At the predicted functional level, differences in the representation of housekeeping enzymes and xenobiotic transformation and stress response pathways were consistent with functions commonly associated with microbial stress responses [104–106]. The two source-derived consortia nevertheless showed contrasting, seed-dependent predicted functional profiles. The salt-marsh-derived consortium showed predicted enrichment in functions associated with defense, osmoregulation, and extracellular macromolecule processing, including the broad-spectrum proteolytic and hydrolytic enzymes serralysin (EC 3.4.24.40) and creatinase (EC 3.5.3.3) (Figure S6), which are annotated as participating in peptide and guanidino compound utilization [107–109]. In contrast, the freshwater-derived consortium showed predicted enrichment in pathways associated with glutathione metabolism and dioxygenase activity, as well as DNA repair pathways. This pattern may reflect greater potential for oxidative stress and xenobiotic response functions [110,111]. The higher predicted representation of taurine/hypotaurine metabolism in the salt-marsh-derived consortium, and its persistence under PFOA exposure, is consistent with a potential role for osmolyte-

associated functions under saline conditions. The surfactant properties of PFOA and its reported effects on membrane permeability provide a possible biological context for this predicted pattern [112]. In particular, hypotaurine acts as an effective scavenger of hydroxyl radicals, neutralizing oxidative damage before it can disable ribosomal function or fragment genomic DNA [113]. Together, these predicted signatures are consistent with greater representation of functions associated with membrane maintenance, ion regulation, and antioxidant defense in the salt-marsh-derived community. These predicted functions describe differences between the two enriched consortia and require direct functional measurements for validation. By contrast, the freshwater-marsh-derived consortium showed higher predicted representation of functions associated with cellular repair and xenobiotic oxidation, including glutathione metabolism, dioxygenase activity (e.g., phthalate 4,5-dioxygenase, EC 1.14.12.7), and DNA repair pathways such as non-homologous end joining (ko03450). Glutathione is the central low-molecular-weight antioxidant in many bacteria and defends against the reactive oxygen species (ROS) generated under PFOA exposure [114]. The higher predicted representation of glutathione metabolism in the freshwater-derived consortium indicates greater inferred potential for glutathione-associated antioxidant functions. In parallel, PFOA-induced oxidative stress and membrane damage have been reported to elevate rates of horizontal gene transfer in adjacent biofilm communities, with possible implications for the spread of resistance traits [84]. The higher predicted representation of oxidative enzymes may reflect broader xenobiotic response potential, even though the C–F backbone of PFOA itself remains recalcitrant to enzymatic attack. Because Tax4Fun2 infers functional potential from 16S rRNA gene profiles, these results are not measurements of pathway expression or biochemical activity. Confirming that these predicted functions reflect active physiological responses would require direct measurements of ROS and glutathione/GSSG ratios, together with metabolomic, transcriptomic, or proteomic analyses. When these ecological patterns are integrated, in the salt-marsh-derived consortium, PFOA may act as a deterministic filter that inhibits sensitive marine-associated taxa, leaving a smaller community characterized by predicted osmolyte management and extracellular proteolysis functions. By contrast, in the freshwater-derived consortium, PFOA may act as a competitive-release disturbance that relieves dominance and is associated with greater predicted representation of functions related to redox buffering, xenobiotic transformation, and DNA repair. The same chemical exposure was therefore associated with different taxonomic, assembly, and predicted functional patterns in the two source-derived consortia.

The community assembly analyses identified different assembly patterns in the two laboratory-enriched consortia under PFOA exposure. Although incubation time drove both systems toward predominantly stochastic assembly by Day 75, the early stages were marked by strong deterministic filtering, and the PFOA treatments showed the strongest signature in the salt-marsh-derived consortium. Heterogeneous selection dominated the response of the salt-marsh-derived consortium, a pattern consistent with high-stress environments in which environmental filters such as salinity and nutrient limitation strongly dictate community membership [115,116]. Deterministic, niche-based selection acts when environmental conditions filter taxa according to their functional traits [117]. In the salt-marsh-derived consortium, PFOA imposed a stronger deterministic signature than in the freshwater-derived consortium, particularly at 1 mg/L, where heterogeneous selection accounted for approximately two-thirds of the assembly process. This pattern indicates stronger filtering in the salt-marsh-derived community under the tested culture conditions, with only a subset of pre-adapted genotypes occupying the resulting niche. Salinity may have contributed to this pattern, but its effect cannot be separated from microbiome source or other differences between the culture conditions. PFOA thus may operate as an additional selective layer on an already-selective abiotic background, intensifying the role of

deterministic processes observed in the βNTI analysis. These results therefore support the view that predicting a community's response to a contaminant requires explicit knowledge of its baseline assembly regime. The present results suggest that responses to the same PFOA exposure may differ between source-derived consortia under their respective culture conditions [118]. A similar shift from stochastic toward deterministic assembly with increasing contaminant load has also been reported in polluted freshwater systems [119]. Importantly, when PFOA-exposed samples were pooled across both enriched consortia, the neutral community model fit collapsed (Figure 5C; $R^2 < 0$), indicating that PFOA-driven selection can override neutral dispersal at the system level. The collapse is a regime shift effect consistent with the dose-amplified deterministic signature observed in the salt-marsh-derived consortium βNTI (Figure 4A), and with the further increase of drift in the freshwater-derived consortium at 10 mg/L. At the lower 1 mg/L exposure, by contrast, the same chemical perturbation produced clearly seed-dependent effects on assembly. This source-dependent contrast was observed within the tested enrichment system and cannot be used to define field-scale toxicity or remediation criteria. The NCM analysis yielded a higher fitted migration parameter for the freshwater-derived consortium than for the salt-marsh-derived consortium. This difference describes the experimental consortia and should not be interpreted as evidence that the corresponding natural freshwater marsh is more open or better connected. This higher connectivity likely underpins the apparent resilience of the freshwater-marsh-derived consortium, because taxa lost to disturbance can be more readily replaced by stochastic immigration. The negative R^2 of the PFOA-pooled NCM fit further indicates that, under PFOA exposure, neutral dispersal alone can no longer explain the occurrence–abundance relationship, consistent with previous observations that environmental stress generally favors pre-tolerant species and reshapes community structure accordingly [120]. In the present case, PFOA acts as a selective agent in addition to the simplified, resource-limited microcosm environment. The magnitude of the deterministic shift associated with PFOA depended on the recipient consortium: the same exposure was associated with a near-neutral perturbation in the freshwater-derived consortium and a stronger selective disturbance in the salt-marsh-derived consortium. The candidate taxa identified in this study are specific to the enriched consortia and require validation in unmanipulated field communities before they can be considered for biomonitoring.

In conclusion, under the tested culture conditions, PFOA produced context-dependent responses in the laboratory-enriched freshwater- and salt-marsh-derived consortia, acting as a near-neutral perturbation in the freshwater-derived consortium and as a strongly selective, niche-based filter in the salt-marsh-derived consortium. Because these consortia were shaped by extraction, defined-media cultivation, and serial transfer, the observed responses should not be extrapolated directly to intact wetland microbial communities under field conditions. The two enriched consortia exhibited contrasting predicted functional profiles, with greater representation of antioxidant defense and DNA repair pathways in the freshwater-derived consortium and of osmolyte management and proteolytic functions in the salt-marsh-derived consortium. These patterns describe contrasting PFOA-associated responses of the two laboratory-enriched, soil-derived microbial consortia under their respective culture conditions and should not be interpreted as differences between intact freshwater marsh and salt marsh microbiomes. In the exploratory alpha diversity analysis, microbial community source and sampling day accounted for most of the observed variation, whereas PFOA concentration showed a nominal overall association only with Shannon diversity. Because interaction terms could not be estimated, the observed source-specific patterns should not be interpreted as confirmatory evidence that PFOA produced opposite diversity responses in the two consortia. Whether this pattern extends to other salt-affected systems requires validation using field samples with accompanying physicochemical measurements.

Because microbiome source and culture salinity were not separated experimentally, their individual contributions to the observed differences cannot be resolved. Within the experimental system, samples from the two PFOA-exposed consortia deviated from the neutral community model prediction, indicating a stronger contribution of selection relative to neutral dispersal under the tested conditions. This pattern should not be extrapolated to ecosystem-level community assembly. The contrasting responses caution against assuming a single microbial response to PFOA across source-derived enriched consortia, although their relevance to field-scale PFAS risk assessment remains to be established. The source-associated taxa identified here are candidates for future validation and should not yet be considered field biomarkers. Similarly, the possible contribution of biomass- or EPS-mediated biosorption requires direct measurement before it can inform the design of PFAS remediation strategies. These findings provide testable hypotheses for future studies of natural attenuation and wetland-based treatment systems but are insufficient to establish their performance in native wetlands. Future work pairing broader taxonomic characterization and time-resolved metatranscriptomics with quantitative fluorine mass balance across replicated field sites will be needed to determine whether these microcosm patterns occur in unmanipulated sediments and whether the candidate taxa can serve as field biomarkers of PFAS exposure.

Supplementary Materials: The following supporting information can be downloaded at: https://www.mdpi.com/article/10.3390/environments13110616/s1. Figure S1: Map of sampling locations along the Neponset River Estuary, Boston Harbor, Massachusetts, USA; Table S1: Alpha-diversity indices for the freshwater-marsh-derived and salt-marsh-derived consortia at each sampling day (Day 0, 25, 50, 75) and PFOA concentration (0, 1, 10 mg/L); Table S2: Top predicted pathways; Table S3: Enzymes of interest; Figure S2: Exploratory additive mixed-effects model analysis of alpha diversity across microbial community sources, PFOA concentrations, and post-enrichment sampling days; Figure S3: Average variation degree (AVD) of microbial-community temporal stability; Figure S4: Supervised partial least squares discriminant analysis (PLS-DA) of microbial community composition across PFOA treatment groups; Figure S5: One-way ANOVA with Tukey–Kramer post-hoc comparisons of additional Tax4Fun2-predicted functional pathway proportions across PFOA concentrations (0, 1, 10 mg/L) and microbial-community source (salt marsh vs. freshwater marsh); Figure S6: Differential enzyme abundance between freshwater- and salt-marsh-derived consortia under PFOA exposure.

Author Contributions: Conceptualization, Y.M. and W.Z.; methodology, Y.M. and T.V.; software, T.V. and M.K.; validation, Y.M., T.V. and W.Z.; formal analysis, T.V., M.K. and M.T.; investigation, T.V., M.K. and M.T.; resources, Y.M. and W.Z.; data curation, T.V., M.K. and M.T.; writing—original draft preparation, T.V., M.K. and M.T.; writing—review and editing, Y.M. and W.Z.; visualization, T.V. and M.T.; supervision, Y.M. and W.Z.; project administration, Y.M. and W.Z.; funding acquisition, Y.M. and W.Z. All authors have read and agreed to the published version of the manuscript.

Funding: This research was funded by Northeastern University New Faculty Startup Funding, and the U.S. Department of War's The Strategic Environmental Research and Development Program (SERDP), award # W912HQ25P0012.

Data Availability Statement: The data presented in this study are available upon request to the corresponding author.

Acknowledgments: The authors thank research facilities at Northeastern University and the University at Albany, SUNY, for microbiological and chemical analyses.

Conflicts of Interest: The authors declare no conflicts of interest.

Abbreviations

The following abbreviations are used in this manuscript:

AMS	Ammonium mineral salts
ANOSIM	Analysis of similarities
ANOVA	Analysis of variance
AVD	Average variation degree
βNTI	Beta-nearest taxon index
CoA	Coenzyme A
DNA	Deoxyribonucleic acid
EC	Enzyme commission
EPS	Extracellular polymeric substances
GTPase	Guanosine triphosphatase
KEGG	Kyoto Encyclopedia of Genes and Genomes
LC–MS/MS	Liquid chromatography-tandem mass spectrometry
LDA	Linear discriminant analysis
LEfSe	Linear discriminant analysis effect size
MPs	Microplastics
MRM	Multiple-reaction monitoring
NCM	Neutral community model
OCPs	Organochlorine pesticides
OD_{600}	Optical density at 600 nm
OTUs	Operational taxonomic units
PBS	Phosphate-buffered saline
PCBs	Polychlorinated biphenyls
PCoA	Principal coordinate analysis
PFASs	Per- and polyfluoroalkyl substances
PFOA	Perfluorooctanoic acid
PLS-DA	Partial least squares discriminant analysis
ROS	Reactive oxygen species
rRNA	Ribosomal ribonucleic acid

References

1. Girones, L.; Oliva, A.L.; Negrin, V.L.; Marcovecchio, J.E.; Arias, A.H. Persistent organic pollutants (POPs) in coastal wetlands: A review of their occurrences, toxic effects, and biogeochemical cycling. *Mar. Pollut. Bull.* **2021**, *172*, 112864. [CrossRef]
2. Mitsch, W.J.; Bernal, B.; Nahlik, A.M.; Mander, Ü.; Zhang, L.; Anderson, C.J.; Jørgensen, S.E.; Brix, H. Wetlands, carbon, and climate change. *Landsc. Ecol.* **2013**, *28*, 583–597. [CrossRef]
3. Zedler, J.B.; Kercher, S. Wetland resources: Status, trends, ecosystem services, and restorability. *Annu. Rev. Environ. Resour.* **2005**, *30*, 39–74. [CrossRef]
4. Guimond, J.; Tamborski, J. Salt marsh hydrogeology: A review. *Water* **2021**, *13*, 543. [CrossRef]
5. Salimi, S.; Almuktar, S.A.; Scholz, M. Impact of climate change on wetland ecosystems: A critical review of experimental wetlands. *J. Environ. Manag.* **2021**, *286*, 112160. [CrossRef]
6. Kirwan, M.L.; Megonigal, J.P. Tidal wetland stability in the face of human impacts and sea-level rise. *Nature* **2013**, *504*, 53–60. [CrossRef]
7. White, E.; Kaplan, D. Restore or retreat? Saltwater intrusion and water management in coastal wetlands. *Ecosyst. Health Sustain.* **2017**, *3*, e01258. [CrossRef]
8. Kirwan, M.L.; Walters, D.C.; Reay, W.G.; Carr, J.A. Sea level driven marsh expansion in a coupled model of marsh erosion and migration. *Geophys. Res. Lett.* **2016**, *43*, 4366–4373. [CrossRef]
9. Montalvo, M.S.; Grande, E.; Braswell, A.E.; Visser, A.; Arora, B.; Seybold, E.C.; Tatariw, C.; Haskins, J.C.; Endris, C.A.; Gerbl, F.; et al. A fresh take: Seasonal changes in terrestrial freshwater inputs impact salt marsh hydrology and vegetation dynamics. *Estuaries Coasts* **2024**, *47*, 2714. [CrossRef]
10. Osland, M.J.; Feher, L.C.; Griffith, K.T.; Cavanaugh, K.C.; Enwright, N.M.; Day, R.H.; Stagg, C.L.; Krauss, K.W.; Howard, R.J.; Grace, J.B.; et al. Climatic controls on the global distribution, abundance, and species richness of mangrove forests. *Ecol. Monogr.* **2017**, *87*, 341–359. [CrossRef]
11. Ballesteros, N.; Páez, L.; Luna, N.; Reina, A.; Urrea, V.; Sánchez, C.; Ramírez, A.; Ramirez, J.D.; Muñoz, M. Characterization of microbial communities in seven wetlands with different anthropogenic burden using Next Generation Sequencing in Bogotá, Colombia. *Sci. Rep.* **2023**, *13*, 16973. [CrossRef]

12. Chapman, S.K.; Hayes, M.A.; Kelly, B.; Langley, J.A. Exploring the oxygen sensitivity of wetland soil carbon mineralization. *Biol. Lett.* **2019**, *15*, 20180407. [CrossRef]
13. Behera, P.; Mahapatra, S.; Mohapatra, M.; Kim, J.Y.; Adhya, T.K.; Raina, V.; Suar, M.; Pattnaik, A.K.; Rastogi, G. Salinity and macrophyte drive the biogeography of the sedimentary bacterial communities in a brackish water tropical coastal lagoon. *Sci. Total Environ.* **2017**, *595*, 472–485. [CrossRef]
14. Bouskill, N.J.; Wood, T.E.; Baran, R.; Ye, Z.; Bowen, B.P.; Lim, H.; Zhou, J.; Van Nostrand, J.D.; Nico, P.; Northen, T.R.; et al. Belowground response to drought in a tropical forest soil. I. changes in microbial functional potential and metabolism. *Front. Microbiol.* **2016**, *7*, 525. [CrossRef]
15. von Rein, I.; Gessler, A.; Premke, K.; Keitel, C.; Ulrich, A.; Kayler, Z.E. Forest understory plant and soil microbial response to an experimentally induced drought and heat-pulse event: The importance of maintaining the continuum. *Glob. Change Biol.* **2016**, *22*, 2861–2874. [CrossRef]
16. Mustafa, G.; Hussain, S.; Liu, Y.; Ali, I.; Liu, J.; Bano, H. Microbiology of wetlands and the carbon cycle in coastal wetland mediated by microorganisms. *Sci. Total Environ.* **2024**, *954*, 175734. [CrossRef]
17. Batanero, G.L.; Green, A.J.; Amat, J.A.; Vittecoq, M.; Suttle, C.A.; Reche, I. Patterns of microbial abundance and heterotrophic activity along nitrogen and salinity gradients in coastal wetlands. *Aquat. Sci.* **2022**, *84*, 22. [CrossRef]
18. Lamers, L.P.; van Diggelen, J.M.; Op den Camp, H.J.; Visser, E.J.; Lucassen, E.C.; Vile, M.A.; Jetten, M.S.; Smolders, A.J.; Roelofs, J.G. Microbial transformations of nitrogen, sulfur, and iron dictate vegetation composition in wetlands: A review. *Front. Microbiol.* **2012**, *3*, 156. [CrossRef]
19. Liu, H.; Zhao, B.; Jin, M.; Wang, R.; Ding, Z.; Wang, X.; Xu, W.; Chen, Q.; Tao, R.; Fu, J. Anthropogenic-induced ecological risks on marine ecosystems indicated by characterizing emerging pollutants in Pearl River Estuary, China. *Sci. Total Environ.* **2024**, *926*, 172030. [CrossRef]
20. Ahrens, L.; Norström, K.; Viktor, T.; Cousins, A.P.; Josefsson, S. Stockholm Arlanda Airport as a source of per- and polyfluoroalkyl substances to water, sediment and fish. *Chemosphere* **2015**, *129*, 33–38. [CrossRef]
21. Prevedouros, K.; Cousins, I.T.; Buck, R.C.; Korzeniowski, S.H. Sources, Fate and Transport of Perfluorocarboxylates. *Environ. Sci. Technol.* **2006**, *40*, 32–44. [CrossRef]
22. Dickman, R.A.; Aga, D.S. A review of recent studies on toxicity, sequestration, and degradation of per- and polyfluoroalkyl substances (PFAS). *J. Hazard. Mater.* **2022**, *436*, 129120. [CrossRef]
23. Pepper, I.L.; Brusseau, M.L.; Prevatt, F.J.; Escobar, B.A. Incidence of PFAS in soil following long-term application of class B biosolids. *Sci. Total Environ.* **2021**, *793*, 148449. [CrossRef]
24. Senevirathna, S.T.M.L.D.; Mahinroosta, R.; Li, M.; KrishnaPillai, K. In situ soil flushing to remediate confined soil contaminated with PFOS- an innovative solution for emerging environmental issue. *Chemosphere* **2021**, *262*, 127606. [CrossRef]
25. Qin, X.D.; Qian, Z.M.; Dharmage, S.C.; Perret, J.; Geiger, S.D.; Rigdon, S.E.; Howard, S.; Zeng, X.W.; Hu, L.W.; Yang, B.Y.; et al. Association of perfluoroalkyl substances exposure with impaired lung function in children. *Environ. Res.* **2017**, *155*, 15–21. [CrossRef]
26. Griffin, E.K.; Aristizabal-Henao, J.; Timshina, A.; Ditz, H.L.; Camacho, C.G.; da Silva, B.F.; Coker, E.S.; Deliz Quiñones, K.Y.; Aufmuth, J.; Bowden, J.A. Assessment of per- and polyfluoroalkyl substances (PFAS) in the Indian River Lagoon and Atlantic coast of Brevard County, FL, reveals distinct spatial clusters. *Chemosphere* **2022**, *301*, 134478. [CrossRef]
27. Li, J.; Sun, J.; Li, P. Exposure routes, bioaccumulation and toxic effects of per-and polyfluoroalkyl substances (PFASs) on plants: A critical review. *Environ. Int.* **2022**, *158*, 106891. [CrossRef]
28. Evich, M.G.; Davis, M.J.; McCord, J.P.; Acrey, B.; Awkerman, J.A.; Knappe, D.R.; Lindstrom, A.B.; Speth, T.F.; Tebes-Stevens, C.; Strynar, M.J. Per-and polyfluoroalkyl substances in the environment. *Science* **2022**, *375*, eabg9065.
29. Kwok, K.Y.; Yamazaki, E.; Yamashita, N.; Taniyasu, S.; Murphy, M.B.; Horii, Y.; Petrick, G.; Kallerborn, R.; Kannan, K.; Murano, K. Transport of perfluoroalkyl substances (PFAS) from an arctic glacier to downstream locations: Implications for sources. *Sci. Total Environ.* **2013**, *447*, 46–55. [CrossRef]
30. Huang, H.; Lyu, X.; Xiao, F.; Fu, J.; Xu, H.; Wu, J.; Sun, Y. Three-year field study on the temporal response of soil microbial communities and functions to PFOA exposure. *J. Hazard. Mater.* **2024**, *476*, 135008. [CrossRef]
31. Panella, M.; Rabadi, A.; Ceja-Vega, J.; Said, J.; Andersen, E.; Mitchell, J.; Ceja, J.; Lee, S. Membrane-modifying effects of perfluoroalkyl substances in model bacterial membranes. *ACS Omega* **2025**, *10*, 39884–39897. [CrossRef]
32. Cai, Y.; Chen, H.; Yuan, R.; Wang, F.; Chen, Z.; Zhou, B. Metagenomic analysis of soil microbial community under PFOA and PFOS stress. *Environ. Res.* **2020**, *188*, 109838. [CrossRef]
33. Qiao, W.; Xie, Z.; Zhang, Y.; Liu, X.; Xie, S.; Huang, J.; Yu, L. Perfluoroalkyl substances (PFASs) influence the structure and function of soil bacterial community: Greenhouse experiment. *Sci. Total Environ.* **2018**, *642*, 1118–1126. [CrossRef]
34. Bao, Y.; Li, B.; Xie, S.; Huang, J. Vertical profiles of microbial communities in perfluoroalkyl substance-contaminated soils. *Ann. Microbiol.* **2018**, *68*, 399–408. [CrossRef]

35. Wu, J.-Y.; Ding, F.-G.; Shen, Z.-W.; Hua, Z.-L.; Gu, L. Linking microbiomes with per- and poly-fluoroalkyl substances (PFASs) in soil ecosystems: Microbial community assembly, stability, and trophic phylosymbiosis. *Chemosphere* **2022**, *305*, 135403. [CrossRef]
36. Wu, J.-Y.; Gu, L.; Hua, Z.-L.; Liang, Z.-Y.; Chu, K.-J.; He, X.-X. Per-, poly-fluoroalkyl substances (PFASs) pollution in benthic riverine ecosystem: Integrating microbial community coalescence and biogeochemistry with sediment distribution. *Chemosphere* **2021**, *281*, 130977. [CrossRef]
37. Xu, B.; Yang, G.; Lehmann, A.; Riedel, S.; Rillig, M.C. Effects of perfluoroalkyl and polyfluoroalkyl substances (PFAS) on soil structure and function. *Soil Ecol. Lett.* **2023**, *5*, 108–117. [CrossRef]
38. Calcagnile, M.; Giuliano, A.; Tredici, M.S.; Gualandris, D.; Rotondo, D.; Calisi, A.; Leo, C.; Martelli, M.; Rocchi, A.; Klint, K.E.; et al. Per- and polyfluoroalkyl substances (PFAS) as environmental drivers of antimicrobial resistance: Insights from genome sequences of Klebsiella grimontii and Citrobacter braakii isolated from contaminated soil. *Environ. Sci. Adv.* **2025**, *4*, 1444–1476. [CrossRef]
39. Jiang, T.; Geisler, M.; Zhang, W.; Liang, Y. Fluoroalkylether compounds affect microbial community structures and abundance of nitrogen cycle-related genes in soil-microbe-plant systems. *Ecotoxicol. Environ. Saf.* **2021**, *228*, 113033. [CrossRef]
40. Zhang, L.; Huang, D.; Zhang, Z.; Liu, X.; Lin, X.; Gao, B.; Liu, Y.; Ma, W.; Zhang, H. Dissection of denitrification pathways and synergistic degradation mechanisms of functional microbial communities under Per- and Polyfluoroalkyl Substances (PFAS) exposure. *Bioresour. Technol.* **2026**, *448*, 134290. [CrossRef]
41. Xu, R.; Tao, W.; Lin, H.; Huang, D.; Su, P.; Gao, P.; Sun, X.; Yang, Z.; Sun, W. Effects of Perfluorooctanoic Acid (PFOA) and Perfluorooctane Sulfonic Acid (PFOS) on Soil Microbial Community. *Microb. Ecol.* **2022**, *83*, 929–941. [CrossRef]
42. Wang, F.; Shih, K. Adsorption of perfluorooctanesulfonate (PFOS) and perfluorooctanoate (PFOA) on alumina: Influence of solution pH and cations. *Water Res.* **2011**, *45*, 2925–2930. [CrossRef]
43. Liang, S.; Li, H.; Wu, H.; Yan, B.; Song, A. Microorganisms in coastal wetland sediments: A review on microbial community structure, functional gene, and environmental potential. *Front. Microbiol.* **2023**, *14*, 1163896. [CrossRef]
44. Webster, G.; O'Sullivan, L.A.; Meng, Y.; Williams, A.S.; Sass, A.M.; Watkins, A.J.; Parkes, R.J.; Weightman, A.J. Archaeal community diversity and abundance changes along a natural salinity gradient in estuarine sediments. *FEMS Microbiol. Ecol.* **2015**, *91*, 1–18. [CrossRef]
45. Zhu, J.; Olsen, C.R. Beryllium-7 atmospheric deposition and sediment inventories in the Neponset River estuary, Massachusetts, USA. *J. Environ. Radioact.* **2009**, *100*, 192–197. [CrossRef]
46. Gardner, G.B.; Chen, R.F.; Berry, A. High-resolution measurements of chromophoric dissolved organic matter (CDOM) in the Neponset River Estuary, Boston Harbor, MA. *Mar. Chem.* **2005**, *96*, 137–154. [CrossRef]
47. Lindahl, V. Improved soil dispersion procedures for total bacterial counts, extraction of indigenous bacteria and cell survival. *J. Microbiol. Methods* **1996**, *25*, 279–286. [CrossRef]
48. Riis, V.; Lorbeer, H.; Babel, W. Extraction of microorganisms from soil: Evaluation of the efficiency by counting methods and activity measurements. *Soil Biol. Biochem.* **1998**, *30*, 1573–1581. [CrossRef]
49. El Mujtar, V.A.; Chirdo, F.; Lagares, A.; Wall, L.; Tittonell, P. Soil bacterial biodiversity characterization by flow cytometry: The bottleneck of cell extraction from soil. *Methods Ecol. Evol.* **2022**, *13*, 1388–1401. [CrossRef]
50. Omer, Z.S.; Tombolini, R.; Gerhardson, B. Plant colonization by pink-pigmented facultative methylotrophic bacteria (PPFMs). *FEMS Microbiol. Ecol.* **2004**, *47*, 319–326. [CrossRef]
51. Kelly, D.P.; Ardley, J.K.; Wood, A.P. Cultivation of methylotrophs. In *Hydrocarbon and Lipid Microbiology Protocols: Isolation and Cultivation*; Springer: Berlin/Heidelberg, Germany, 2014; pp. 197–229.
52. Henson, M.W.; Pitre, D.M.; Weckhorst, J.L.; Lanclos, V.C.; Webber, A.T.; Thrash, J.C. Artificial Seawater Media Facilitate Cultivating Members of the Microbial Majority from the Gulf of Mexico. *mSphere* **2018**, *3*, 00415–00418. [CrossRef]
53. Cunliffe, M. Purine catabolic pathway revealed by transcriptomics in the model marine bacterium Ruegeria pomeroyi DSS-3. *FEMS Microbiol. Ecol.* **2016**, *92*, fiv150. [CrossRef]
54. Kunacheva, C.; Fujii, S.; Tanaka, S.; Seneviratne, S.; Lien, N.P.H.; Nozoe, M.; Kimura, K.; Shivakoti, B.R.; Harada, H. Worldwide surveys of perfluorooctane sulfonate (PFOS) and perfluorooctanoic acid (PFOA) in water environment in recent years. *Water Sci. Technol.* **2012**, *66*, 2764–2771. [CrossRef]
55. Goldford, J.E.; Lu, N.; Bajic, D.; Estrela, S.; Tikhonov, M.; Sanchez-Gorostiaga, A.; Segre, D.; Mehta, P.; Sanchez, A. Emergent simplicity in microbial community assembly. *Science* **2018**, *361*, 469–474. [CrossRef]
56. Zegeye, E.K.; Brislawn, C.J.; Farris, Y.; Fansler, S.J.; Hofmockel, K.S.; Jansson, J.K.; Wright, A.T.; Graham, E.B.; Naylor, D.; McClure, R.S.; et al. Selection, Succession, and Stabilization of Soil Microbial Consortia. *mSystems* **2019**, *4*. [CrossRef]
57. Wang, H.; Gu, Y.; Zhou, W.; Zhao, D.; Qiao, Z.; Zheng, J.; Gao, J.; Chen, X.; Ren, C.; Xu, Y. Adaptability of a Caproate-Producing Bacterium Contributes to Its Dominance in an Anaerobic Fermentation System. *Appl. Environ. Microbiol.* **2021**, *87*, e0120321. [CrossRef]
58. Korenblum, E.; Jimenez, D.J.; van Elsas, J.D. Succession of lignocellulolytic bacterial consortia bred anaerobically from lake sediment. *Microb. Biotechnol.* **2016**, *9*, 224–234. [CrossRef]

59. Xun, W.; Liu, Y.; Li, W.; Ren, Y.; Xiong, W.; Xu, Z.; Zhang, N.; Miao, Y.; Shen, Q.; Zhang, R. Specialized metabolic functions of keystone taxa sustain soil microbiome stability. *Microbiome* **2021**, *9*, 35. [CrossRef]
60. Zhang, D.; Zhang, W.; Liang, Y. Bacterial community in a freshwater pond responding to the presence of perfluorooctanoic acid (PFOA). *Environ. Technol.* **2020**, *41*, 3646–3656. [CrossRef]
61. Laine, M.B.; Vesamäki, J.S.; Puupponen, V.-M.; Tiirola, M.; Taipale, S.J. Comparing the ecotoxicological effects of perfluorooctanoic acid (PFOA) and perfluorohexanoic acid (PFHxA) on freshwater microbial community. *Front. Environ. Sci.* **2022**, *10*, 888171. [CrossRef]
62. Alden, L.; Demoling, F.; Baath, E. Rapid method of determining factors limiting bacterial growth in soil. *Appl. Environ. Microbiol.* **2001**, *67*, 1830–1838. [CrossRef]
63. Bartelme, R.P.; Custer, J.M.; Dupont, C.L.; Espinoza, J.L.; Torralba, M.; Khalili, B.; Carini, P. Influence of substrate concentration on the culturability of heterotrophic soil microbes isolated by high-throughput dilution-to-extinction cultivation. *mSphere* **2020**, *5*. [CrossRef]
64. Kharel, M.; Tian, M.; Vu, T.; Miao, Y.; Zhang, W. PFAS in plant-biosolids-soil systems: Distribution, fractionation, and effects on soil microbial communities. *J. Hazard. Mater.* **2025**, *497*, 139754. [CrossRef]
65. Schnecker, J.; Böckle, T.; Horak, J.; Martin, V.; Sandén, T.; Spiegel, H. Improving measurements of microbial growth, death, and turnover by accounting for extracellular DNA in soils. *Soil* **2024**, *10*, 521–531. [CrossRef]
66. Bairoliya, S.; Koh Zhi Xiang, J.; Cao, B. Extracellular DNA in Environmental Samples: Occurrence, Extraction, Quantification, and Impact on Microbial Biodiversity Assessment. *Appl. Environ. Microbiol.* **2022**, *88*, e0184521. [CrossRef]
67. Schloss, P.D. Reintroducing mothur: 10 years later. *Appl. Environ. Microbiol.* **2020**, *86*, e02343-19. [CrossRef]
68. Miao, Y.; Zhou, T.; Zheng, X.; Mahendra, S. Investigating biodegradation of 1, 4-dioxane by groundwater and soil microbiomes: Insights into microbial ecology and process prediction. *ACS EST Water* **2023**, *4*, 1046–1060. [CrossRef]
69. Yu, C.; Zhu, Z.; Meng, K.; Zhang, H.; Xu, M. Unveiling the impact and mechanisms of Cd-driven ecological assembly and coexistence of bacterial communities in coastal sediments of Yellow Sea. *J. Hazard. Mater.* **2023**, *460*, 132309. [CrossRef]
70. Wemheuer, F.; Taylor, J.A.; Daniel, R.; Johnston, E.; Meinicke, P.; Thomas, T.; Wemheuer, B. Tax4Fun2: A R-based tool for the rapid prediction of habitat-specific functional profiles and functional redundancy based on 16S rRNA gene marker gene sequences. *BioRxiv* **2018**, *preprint*. [CrossRef]
71. Miao, Y.; Heintz, M.B.; Bell, C.H.; Johnson, N.W.; Polasko, A.L.; Favero, D.; Mahendra, S. Profiling microbial community structures and functions in bioremediation strategies for treating 1, 4-dioxane-contaminated groundwater. *J. Hazard. Mater.* **2021**, *408*, 124457. [CrossRef]
72. Stegen, J.C.; Lin, X.; Konopka, A.E.; Fredrickson, J.K. Stochastic and deterministic assembly processes in subsurface microbial communities. *ISME J.* **2012**, *6*, 1653–1664. [CrossRef]
73. Sloan, W.T.; Lunn, M.; Woodcock, S.; Head, I.M.; Nee, S.; Curtis, T.P. Quantifying the roles of immigration and chance in shaping prokaryote community structure. *Environ. Microbiol.* **2006**, *8*, 732–740. [CrossRef]
74. Hubbell, S.P. The unified neutral theory of biodiversity and biogeography. In *The Unified Neutral Theory of Biodiversity and Biogeography*; Princeton University Press: Princeton, NJ, USA, 2011.
75. Ju, F.; Lau, F.; Zhang, T. Linking microbial community, environmental variables, and methanogenesis in anaerobic biogas digesters of chemically enhanced primary treatment sludge. *Environ. Sci. Technol.* **2017**, *51*, 3982–3992. [CrossRef]
76. McMurdie, P.J.; Holmes, S. phyloseq: An R package for reproducible interactive analysis and graphics of microbiome census data. *PLoS ONE* **2013**, *8*, e61217. [CrossRef]
77. Segata, N.; Izard, J.; Waldron, L.; Gevers, D.; Miropolsky, L.; Garrett, W.S.; Huttenhower, C. Metagenomic biomarker discovery and explanation. *Genome Biol.* **2011**, *12*, R60. [CrossRef]
78. Miao, Y.; Johnson, N.W.; Heck, K.; Guo, S.J.; Powell, C.D.; Phan, T.; Gedalanga, P.B.; Adamson, D.T.; Newell, C.J.; Wong, M.S.; et al. Microbial responses to combined oxidation and catalysis treatment of 1,4-dioxane and co-contaminants in groundwater and soil. *Front. Environ. Sci. Eng.* **2018**, *12*, 2. [CrossRef]
79. Baabish, A.; Sobhanei, S.; Fiedler, H. Priority perfluoroalkyl substances in surface waters-A snapshot survey from 22 developing countries. *Chemosphere* **2021**, *273*, 129612. [CrossRef]
80. Biden, J. *Final PFAS National Primary Drinking Water Regulation*; United States Environmental Protection Agency: Washington, DC, USA, 2024; Volume 1, pp. 1–28.
81. Liu, G.; Zhang, S.; Yang, K.; Zhu, L.; Lin, D. Toxicity of perfluorooctane sulfonate and perfluorooctanoic acid to Escherichia coli: Membrane disruption, oxidative stress, and DNA damage induced cell inactivation and/or death. *Environ. Pollut.* **2016**, *214*, 806–815. [CrossRef]
82. Yan, W.; Qian, T.; Zhang, L.; Wang, L.; Zhou, Y. Interaction of perfluorooctanoic acid with extracellular polymeric substances-Role of protein. *J. Hazard. Mater.* **2021**, *401*, 123381. [CrossRef]
83. Penland, T.N.; Cope, W.G.; Kwak, T.J.; Strynar, M.J.; Grieshaber, C.A.; Heise, R.J.; Sessions, F.W. Trophodynamics of per-and polyfluoroalkyl substances in the food web of a large Atlantic slope river. *Environ. Sci. Technol.* **2020**, *54*, 6800–6811. [CrossRef]

84. Pourrostami Niavol, K.; Achary, M.P.; Suri, R.P.S.; Andaluri, G. The short-term impact of PFAS exposure on a moving bed biofilm reactor (MBBR): Performance evaluation and the fate of antibiotic resistance genes (ARGs). *J. Water Process Eng.* **2025**, *81*, 109285. [CrossRef]
85. Ha, G.-S.; Sim, M.-G.; Jeon, B.-H.; Baek, G. Bioremediation of perfluorooctanoic acid using microalgae with a transcriptomic approach. *J. Hazard. Mater.* **2026**, *515*, 143235. [CrossRef]
86. Guo, C.; Ahrens, L.; Bertilsson, S.; Coolen, M.J.L.; Tang, J. Microcosm experiment to test bacterial responses to perfluorooctanoate exposure. *Sci. Total Environ.* **2023**, *857*, 159685. [CrossRef]
87. Tang, Z.; Vogel, T.M.; Wang, Q.; Wei, C.; Ali, M.; Song, X. Microbial defluorination of TFA, PFOA, and HFPO-DA by a native microbial consortium under anoxic conditions. *J. Hazard. Mater.* **2024**, *465*, 133217. [CrossRef]
88. Santillan, E. *Disturbance-Performance-Diversity Relationships and Microbial Ecology in Bioreactors for Wastewater Treatment*; ProQuest Dissertations & Theses: Ann Arbor, MI, USA, 2018.
89. Ares, J. Time and space issues in ecotoxicology: Population models, landscape pattern analysis, and long-range environmental chemistry. *Environ. Toxicol. Chem.* **2003**, *22*, 945–957. [CrossRef]
90. Dini-Andreote, F.; de Cássia Pereira e Silva, M.; Triadó-Margarit, X.; Casamayor, E.O.; van Elsas, J.D.; Salles, J.F. Dynamics of bacterial community succession in a salt marsh chronosequence: Evidences for temporal niche partitioning. *ISME J.* **2014**, *8*, 1989–2001. [CrossRef]
91. Jiao, S.; Zhang, Z.; Yang, F.; Lin, Y.; Chen, W.; Wei, G. Temporal dynamics of microbial communities in microcosms in response to pollutants. *Mol. Ecol.* **2017**, *26*, 923–936. [CrossRef]
92. Huang, S.; Pilloni, G.; Key, T.A.; Jaffé, P.R. Defluorination of various perfluoro alkyl acids and selected PFOA and PFOS monomers by Acidimicrobium sp. Strain A6 enrichment cultures. *J. Hazard. Mater.* **2024**, *480*, 136426. [CrossRef]
93. Kang, Y.; Guo, Z.; Ma, H.; Wu, H.; Zhang, J. Enhanced removal of perfluorooctanoic acid (PFOA) and perfluorooctane sulfonate (PFOS) in constructed wetlands: Iron cycling and microbial mechanisms. *ACS EST Water* **2023**, *3*, 287–297. [CrossRef]
94. Frimmersdorf, E.; Horatzek, S.; Pelnikevich, A.; Wiehlmann, L.; Schomburg, D. How *Pseudomonas aeruginosa* adapts to various environments: A metabolomic approach. *Environ. Microbiol.* **2010**, *12*, 1734–1747. [CrossRef]
95. Akkaya, Ö.; Pérez-Pantoja, D.R.; Calles, B.; Nikel, P.I.; de Lorenzo, V. The metabolic redox regime of *Pseudomonas putida* tunes its evolvability toward novel xenobiotic substrates. *mBio* **2018**, *9*. [CrossRef]
96. MacLean, A.; Bley, A.M.; Appanna, V.P.; Appanna, D.V.D. Metabolic manipulation by *Pseudomonas fluorescens*: A powerful stratagem against oxidative and metal stress. *J. Med. Microbiol.* **2020**, *69*, 339–346. [CrossRef]
97. Ambreetha, S.; Zincke, D.; Balachandar, D.; Mathee, K. Genomic and metabolic versatility of *Pseudomonas aeruginosa* contributes to its inter-kingdom transmission and survival. *J. Med. Microbiol.* **2024**, *73*, 001791. [CrossRef]
98. Zeng, Z.; Li, L.; Wang, H.; Tao, Y.; Lv, Z.; Wang, F.; Wang, Y. Oxidative adaptations in prokaryotes imply the oxygenic photosynthesis before crown-group Cyanobacteria. *PNAS Nexus* **2025**, *4*, pgaf035. [CrossRef]
99. Neumann, H.; Bode-Kirchhoff, A.; Madeheim, A.; Wetzel, A. Toxicity testing of heavy metals with the Rhizobium-legume symbiosis: High sensitivity to cadmium and arsenic compounds. *Environ. Sci. Pollut. Res.* **1998**, *5*, 28–36. [CrossRef]
100. Fox, J.E.; Gulledge, J.; Engelhaupt, E.; Burow, M.E.; McLachlan, J.A. Pesticides reduce symbiotic efficiency of nitrogen-fixing rhizobia and host plants. *Proc. Natl. Acad. Sci. USA* **2007**, *104*, 10282–10287. [CrossRef]
101. Rathjen, J.; Ryder, M.; Riley, I.; Lai, T.; Denton, M. Impact of seed-applied pesticides on rhizobial survival and legume nodulation. *J. Appl. Microbiol.* **2020**, *129*, 389–399. [CrossRef]
102. Wang, H.; Li, Y.; Chen, H.; Yu, P.; Shi, B.; Alvarez, P.J.J. Perfluorooctanoic acid can increase biofilm resilience and virulence in drinking water distribution systems. *Environ. Sci. Technol.* **2025**, *59*, 21028–21038. [CrossRef]
103. Li, B.; Feng, L.; Zhang, J.; Giannakis, S. PFOA and a dash of aluminum: The perfect recipe for growing drug-resistant biofilms in urban water supply. *J. Hazard. Mater.* **2025**, *497*, 139660. [CrossRef]
104. Guan, N.; Li, J.; Shin, H.-d.; Du, G.; Chen, J.; Liu, L. Microbial response to environmental stresses: From fundamental mechanisms to practical applications. *Appl. Microbiol. Biotechnol.* **2017**, *101*, 3991–4008. [CrossRef]
105. Marles-Wright, J.; Lewis, R.J. Stress responses of bacteria. *Curr. Opin. Struct. Biol.* **2007**, *17*, 755–760. [CrossRef]
106. Gottesman, S. Trouble is coming: Signaling pathways that regulate general stress responses in bacteria. *J. Biol. Chem.* **2019**, *294*, 11685–11700. [CrossRef]
107. Sariaslani, F.S. Microbial cytochromes P-450 and xenobiotic metabolism. *Adv. Appl. Microbiol.* **1991**, *36*, 133–178. [CrossRef]
108. Marghade, D.T.; Chahande, A.D.; Tiwari, M.S.; Patil, P.D. Microbial degradation of xenobiotic compounds. In *Recent Advances in Microbial Degradation*; Springer: Berlin/Heidelberg, Germany, 2021; pp. 173–217.
109. McLean, K.J.; Leys, D.; Munro, A.W. Microbial cytochromes P450. In *Cytochrome P450: Structure, Mechanism, and Biochemistry*; Springer: Berlin/Heidelberg, Germany, 2015; pp. 261–407.
110. Rath, S.; Das, S. Oxidative stress-induced DNA damage and DNA repair mechanisms in mangrove bacteria exposed to climatic and heavy metal stressors. *Environ. Pollut.* **2023**, *339*, 122722. [CrossRef]

111. Chao, Y.; Ma, L.; Yang, Y.; Ju, F.; Zhang, X.-X.; Wu, W.-M.; Zhang, T. Metagenomic analysis reveals significant changes of microbial compositions and protective functions during drinking water treatment. *Sci. Rep.* **2013**, *3*, 3550. [CrossRef]
112. Chen, C.; Fang, Y.; Cui, X.; Zhou, D. Effects of trace PFOA on microbial community and metabolisms: Microbial selectivity, regulations and risks. *Water Res.* **2022**, *226*, 119273. [CrossRef]
113. Yancey, P.H. Organic osmolytes as compatible, metabolic and counteracting cytoprotectants in high osmolarity and other stresses. *J. Exp. Biol.* **2005**, *208*, 2819–2830. [CrossRef]
114. Costa, B.F.; Sawaya, C.; Buren, J.V.; Smith, A.L. Investigating anaerobic digestion microbiome resilience to high PFOA and PFOS mixtures during cometabolism. *Bioresour. Technol.* **2025**, *435*, 132877. [CrossRef]
115. Guo, L.; Fang, H.; Ding, Y.; An, C.; Yang, N. Microbial community assembly mechanisms of groundwater under salinity–oxygen stress in the Golmud River Watershed, Northwest China. *Life* **2025**, *15*, 1301. [CrossRef]
116. Zhu, P.; Wang, Y.; Sheng, W.; Yu, M.; Wei, W.; Sun, W.; Gao, J.; Xu, Z.; Cao, M.; Wang, Y. Salinity effect on soil bacterial and archaeal diversity and assembly in phragmites australis salt marshes in the Qaidam Basin, China. *Microorganisms* **2025**, *13*, 1253. [CrossRef]
117. Zhou, J.; Ning, D. Stochastic community assembly: Does it matter in microbial ecology? *Microbiol. Mol. Biol. Rev.* **2017**, *81*, 10. [CrossRef]
118. Zhang, X.; Johnston, E.R.; Liu, W.; Li, L.; Han, X. Environmental changes affect the assembly of soil bacterial community primarily by mediating stochastic processes. *Glob. Change Biol.* **2016**, *22*, 198–207. [CrossRef]
119. Tai, X.; Li, R.; Zhang, B.; Yu, H.; Kong, X.; Bai, Z.; Deng, Y.; Jia, L.; Jin, D. Pollution gradients altered the bacterial community composition and stochastic process of rural polluted ponds. *Microorganisms* **2020**, *8*, 311. [CrossRef]
120. Ning, D.; Wang, Y.; Fan, Y.; Wang, J.; Van Nostrand, J.; Wu, L.; Zhang, P.; Curtis, D.; Tian, R.; Lui, L.; et al. Environmental stress mediates groundwater microbial community assembly. *Nat. Microbiol.* **2024**, *9*, 490–501. [CrossRef]

Disclaimer/Publisher's Note: The statements, opinions and data contained in all publications are solely those of the individual author(s) and contributor(s) and not of MDPI and/or the editor(s). MDPI and/or the editor(s) disclaim responsibility for any injury to people or property resulting from any ideas, methods, instructions or products referred to in the content.